QUE PROPERTY - REPORT ON 2020 AIRBORNE GEOPHYSICAL SURVEY

QUIET LAKE, YUKON TERRITORY

WHITEHORSE MINING DISTRICT

NTS 105C-14 / UTM 604993 E - 6754257 N / WGS 84 / ZONE 8

WORK PERFORMED MAY 25-26, 2020.

CLAIM OWNERS – NOKUYUKON HOLDINGS LTD, STUHINI EXPLORATION LTD, MARK LINDSAY, JOANNE MCDOUGALL

Mark Lindsay
Nokuyukon Holdings Ltd
April 2021

TABLE of CONTENTS

COVER PHOTO: SkyTEM airborne survey instrument – Que 2020.

QUE SUMMARY

An airborne survey was carried out for Stuhini Exploration Ltd. over the Que property in May 2020. SkyTEM, a geophysical survey company based in Denmark was contracted to conduct the survey.

The helicopter-borne aeromagnetic and magnetic survey was designed to map the extent of magnetic and electromagnetic anomalies that were seen in a previous airborne survey that was flown in 2004.

Magnetic and electromagnetic data was collected during the survey. SkyTEM collected a total of 431 line / kilometers of data between May 25 and May 26, 2020. The airborne survey covered an area of 10 X 7.5 kilometers. Grid line spacing was 200 meters and the survey elevation was 40 meters.

A copy of the final report supplied by SkyTEM Canada Inc. is in Appendix 2.

LOCATION and ACCESS

Figure 1

The Que Property is in the Yukon Territory in northern Canada (fig. 1).

The target is located in south-central Yukon near the south end of Quiet Lake (fig. 2) on NTS mapsheet 105C 14 (fig. 3).

The target is within the Whitehorse Mining District. The approximate geographical center for the area would be located at UTM 604993 E / 6754257 N

Figure 2

The Que Project is located approximately 110 kilometers east of the city of Whitehorse and is accessible by helicopter from that location.

The area is also accessible by major roads from Whitehorse over roughly 180 kilometers.

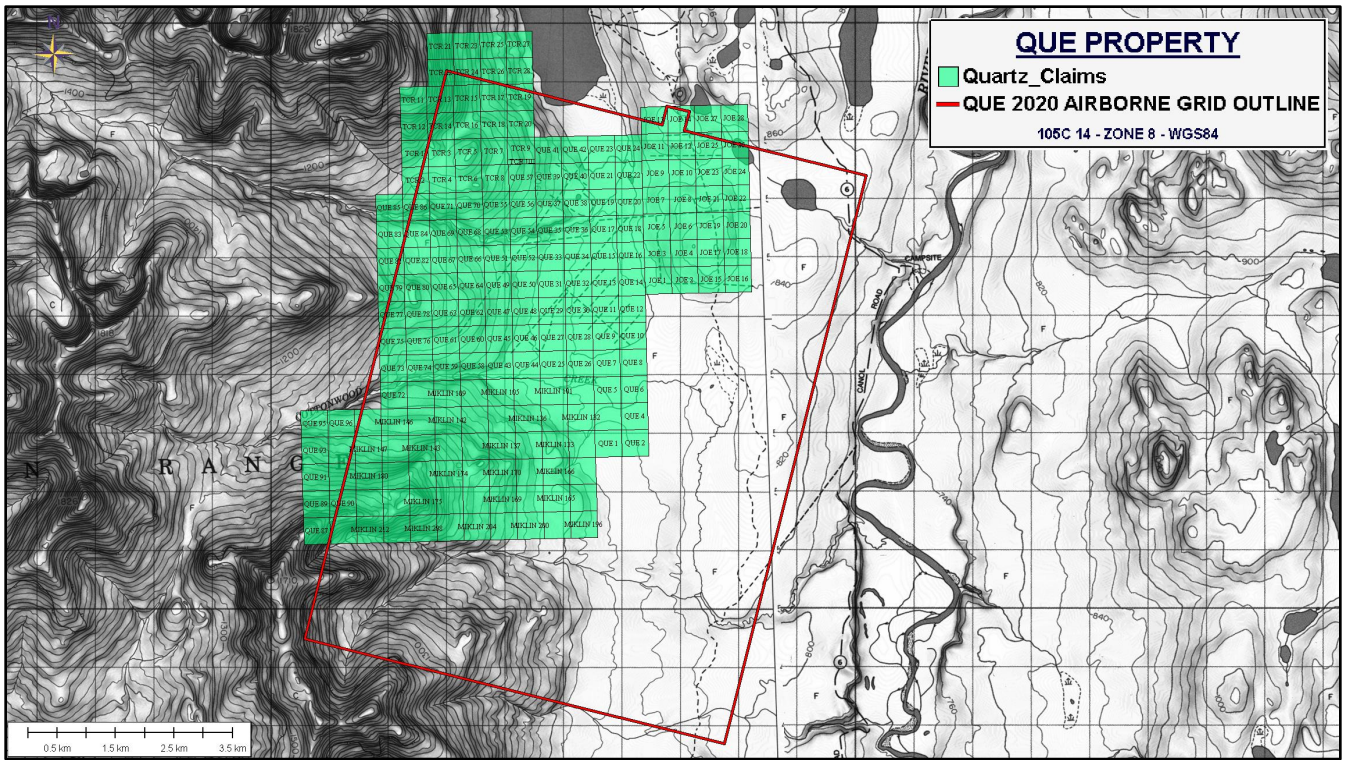

Figure 3

PHYSIOGRAPHY, VEGETATION and CLIMATE

The Que property is in a heavily forested area of low rolling hills to mountainous terrain. The greater part of the target area is below the tree-line boundary (1220m). The highest point in the area of interest is approximately 1519 m.

Drainage in the area is good. Local creeks have a continuous supply of water during the spring and summer months.

Vegetation in the area is dense. Willow, Black Spruce and Lodgepole Pine trees are found throughout the area. Moss and long grasses are also abundant.

The terrain is generally boggy and swampy in the eastern parts of the area. Higher and drier ground (mountain slopes) is found in the western and central parts of the property.

The climate of the area is typical of the interior continental region at this latitude. Winters are long with short hours of daylight and average daily temperatures of –20 Celsius. Summers are pleasant and warm with long days (20 hours of daylight on June 21), although it can be quite rainy at times. The average summer temperature is 19 Celsius with highs ranging into the low 30's.

PROPERTY and CLAIM STATUS

Stuhini Exploration Ltd controls the 204 mineral claims (fig.3) that make up the Que property, which are immediately south of the south end of Quiet Lake, Yukon. The claims cover a total of 4,243 Ha.

GEOLOGY

Que exists within the pericratonic Yukon Tanana Terrane.

The Que property does not have good rock exposure for the greater part of its extent, and as a result the area has not been mapped at scales greater than 1:250,000, but according to the Yukon Geological Survey (who paid a 2-day visit to the property in 2004) the area is underlain by Early to Mid-Paleozoic sedimentary, metasedimentary, and metavolcanic basement rocks. These assemblages have been intruded by ultramafic and felsic rock units.

Paleozoic felsic volcanic rocks (rhyolite) are found along a ridge in the southwest part of the property.

The Cretaceous Quiet Lake Batholith (QLB) intrudes the western portion of the property, but it is not well exposed in outcrop on the property.

A large Paleozoic ultramafic intrusion is inferred (from magnetics) to exist over the north central part of the property. A smaller, potentially related, ultramafic intrusion is found in the south-central part of the property.

HISTORICAL EXPLORATION

The general area of the Que property has been explored intermittently since prospectors first ascended the Big Salmon River to Quiet Lake in the late 1800's in their search for placer gold deposits. The few who prospected this part of the territory recognized the mineral potential and settled in the area. A few creeks in the region produced placer gold and men built small settlements around their discoveries. Cottonwood Creek, which flows through the central part of the Que claim block, was the site of one such settlement.

Gold was discovered on Cottonwood Creek in the late 1800's. At its height the settlement at Cottonwood Creek had approximately 7-9 cabins. It appears that a fire burnt down all of the cabins sometime in the early 1900's. A lone prospector was living and mining on the creek as late as 1925. Equipment found at the prospector's cabin suggests that he was engaged in placer and hard-rock gold mining. Another prospector was documented by the Geological Survey of Canada (GSC) to be living (and potentially hard-rock mining) on the south-west shore of Quiet Lake in 1935.

In the mid 1960's modern interest in the Quiet Lake area began when a large rust zone (Camp Gossan) was discovered by individuals (M. Croider & R.J. Lindsay) who were salvaging pipe from the 1940's Canol Road pipeline. It was later revealed that the US Army had also recorded finding a large area of rust at mile 39.5, while building the original Canol Road. Two other large rust zones (L8 & L52) were subsequently found. Mineral exploration was conducted in the area up to 1978. There have been limited amounts of exploration in the area since that time.

DETAILS of PREVIOUS WORK

Most of the following exploration activities can be found in assessment reports for map-sheet 105C-14 at the Yukon Government Resource Library in Whitehorse.

1966 Newmont Geochemical / Magnetic Survey – A geochemical and magnetic survey by Newmont Mining Corporation 3 kilometers southeast of Quiet Lake.

1968 Airborne Geophysical Survey – A 1968 early time domain airborne electromagnetic (EM) /magnetic (Mag) survey over a section of the QL area.

1968/69 Reconnaissance Geophysical Surveys – Several reconnaissance ground EM, Mag and IP surveys were conducted over sections of the QL area in the late 1960's to investigate isolated conductors identified from the 1968 airborne survey.

1968/69 Reconnaissance Soil Surveys – Three reconnaissance geochemical surveys were carried out over parts of QL. A geochemistry survey for nickel, copper, lead, and zinc was carried out over two grids in the summer of 1968, and a detailed survey for nickel and copper was conducted over a centrally located grid in 1969.

1970's Diamond Drilling - In the fall of 1972 a diamond drilling program was conducted over a large IP anomaly that was identified on one of the property Grids. A Wisconsin powered Longyear Diamond Drill was brought onto the property and three short (AQ) holes were drilled. The first two holes were drilled at 50°. The deepest vertical depth penetration was hole #1 at 78 meters. That hole intersected highly distorted, intensely banded argillite over much of its entire 102-meter length. Sulfides encountered were pyrite, pyrrhotite and minor chalcopyrite and galena. Hole #2 intersected ultramafic at 31 meters and ended in the ultramafic at 77 meters. Hole #3 was 91 meters long. It encountered mainly amphibolite but was not logged. Disseminated sulfides included pyrrhotite and pyrite (up to 10% combined) with some chalcopyrite and galena encountered in the drilling. *In 1983 a section of Hole #1 was re-assayed and reported to have 4 meters of 1.1 g/t Au & 9.3g/t Ag. The drill hole was collared 35 m off the edge of an EM anomaly discovered during the 2004 airborne. The trajectory of the hole was such that it drilled 180°away from the EM target.*

2003 Soil Sample Program - Recon soil sampling was carried out along an isolated ridge in the south western part of the QL Project area. Approximately 144 samples (fig.8) were collected in the area known as Kingdome Ridge. Many of the samples were anomalous in Au, Ag & Cu. The program identified an anomalous trend along the ridge with samples returning values up to 957 ppb gold and 442 ppm Cu. While prospecting the area a rhyolite rock (with quartz veining) was sampled and returned values up to 15 g/t gold.

2003 Geophysics Program - In 2003 a ground truthing EM and Mag survey was conducted over a known (1968) airborne EM / Mag anomaly. The surveys identified a distinct EM anomaly with a relatively low magnetic signature along a linear feature that was interpreted as a fault. Mike Power (Aurora Geosciences) thought the conductor had the characteristics of a massive sulfide horizon and it warranted drilling. The survey also found a large magnetic anomaly situated between two gossan zones in the area. The magnetic anomaly appeared to have a weak associated EM response of a flat lying conductor, but the orientation and size of the grid, prevented it from receiving adequate coverage to make this determination.

2003 Drill Program - In November 2003, the EM/Mag anomaly that was discovered earlier in the fall was drilled. The drill hole was not logged (because the core was lost), but preliminary examinations of the core identified several sections of fractured and brecciated metasedimentary and felsic metavolcanic rocks carrying considerable amounts of sulfide. Pyrite, in semi-massive and disseminated amounts appeared to be the only sulfide mineral within the drill hole. Assays of the core returned low precious and base metal values. The drill results, although barren of precious metals, were encouraging due to the significant pyrite.

2004 Airborne Geophysics Survey – A Hummingbird airborne EM, magnetic and radiometric survey was conducted by McPhar Ltd. over the Que property. A total of 604-line km of geophysical data were acquired. Several strong EM anomalies were found.

RESULTS AND DISCUSSION

The 2020 airborne data has revealed many strong electromagnetic (EM) and magnetic (Mag) anomalies, some of which are coincident over the top of each other. Many of the EM anomalies appear to be associated with the inferred contact of the large ultramafic rock unit in the northern part of the property. An inferred fault structure runs in a NW-SE direction along the south-west margin of the ultramafic.

Along the south-central part of the property a large EM anomaly is found fully encapsulated by a strong magnetic anomaly and over an area known to host another (smaller) ultramafic intrusion. This anomaly is immediately south of another important fault that trends in a SW-NE direction.

A string of individual EM anomalies exists directly over the SW-NE fault mentioned above. This set of EM anomalies is the strongest on the property and are coincidental with weaker Mag anomaly zones. It is interesting that one of these EM anomalies is distinctly pod shaped, is of relatively large size (~200m in diameter) and appears to be a stand-alone anomaly at the end of a trend.

CONCLUSIONS

The Que property exist over an area of diverse geology with potentially important structural features.

Several EM conductors and coincidental magnetic anomalies have been defined by an airborne geophysical survey conducted over the target area in 2020.

Initial assessment of the 2020 airborne survey data and of the known geology suggests that the Que property should receive more intensive ground geological and geochemical investigations to determine the nature of the numerous coincidental electromagnetic and magnetic anomalies that exist over the area.

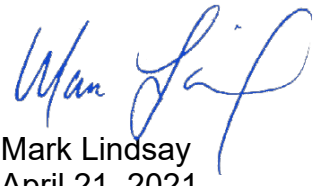

Mark Lindsay
April 21, 2021

STATEMENT OF EXPENDITURES

Yukon

QUARTZ RENEWAL NUMBER

STATEMENT OF EXPENDITURES

This form is to be submitted to the Mining Recorder with the renewal application form when requesting that actual costs be considered for representation work assessment credit at the discretion of the Mining Recorder.

Applicant Name:	**Mark Lindsay**	
Company Name:	**Stuhini Exploration Ltd**	
Work Dates:	25-May-2020 (*1st day of Work*)	26-May-20 (*Last day of Work*)

Claim Names & Grant Numbers:

All TCR, Miklin, Joe and Que claims found on mapsheet 105C-14.

Eligible Expenses — *Please refer to the appropriate Schedule of Representation Work, Prospecting Lease Guidelines, YMIP Rate Guidelines, and/or YG Third Party Rental Book available on-line. Provide photocopies of receipts and/or invoices.*

Personnel Expenses

Employee Full Name and Duties	*Hourly/Daily*	*Qty*	*Pay Rate*	*Total Expenditure*
	Daily Ra			
	Hourly F			
	Daily Ra			
	Daily Ra			

Equipment Description (Receipt Provided)	Owned / Rented	Rates* Cost	Wet/Dry Rate	Daily/Hourly Rate	Number of Days	*Total Expenditure*
	Rented		Dry	Hourly Rate		
				Hourly Rate		
	Rented					
	Owned					

Other Eligible Expenses - Please provide further details:	
SKYTEM AIRBORNE GEOPHYSICS SURVEY	$ 94,889.16

Personnel Expenses Sub-Total:	**$ 0.00**
Equipment Sub-Total:	**$ 0.00**
Other Expenses Sub-Total:	**$ 94,889.16**
TOTAL EXPENSES CLAIMED:	**$ 94,889.16**

Stuhini Exploration Ltd.
1245 West Broadway
Ste. 105
Vancouver, BC V6C 3E8

Att.: Mr.David O'Brien, President & CEO

SkyTEM Canada Inc.
794 Warwick St.
Woodstock, ON N4S 4R1

info@skytem.com
www.skytem.com

HST# : 855492716 RT 0001

INVOICE

Date of invoice: June 30. 2020
Date of payment: June 30, 2020

Your ref.
Survey area Que area, Yukon and Ruby area, BC
Our ref. Q1313 rev.3
Our Invoice No 1364

Final Invoice covering a Helicopter Transient Electromagnetic and Magnetic survey.
Balance remaining upon delivery of the final products.

Description	Percentage	Qty	Unit	Unit price	Amount	
Survey preparation, navigation planning, mobilization and demobilization of equipment, helicopter and crew to survey location	100%	1		30,000.00	30,000.00	CAD 50%
Line kilometer costs including all processing of data and delivery of final report - (line kilometer rate $185.10). Que area	100%	431.6	lkm	185.10	79,889.16	CAD

STATEMENT OF QUALIFICATIONS

I, G. Mark Lindsay hereby certify that:

I am a prospector and President of Nokuyukon Holdings Ltd of Whitehorse, Yukon.

I also currently work for Stuhini Exploration Ltd (TSX-V: STU) of Vancouver, BC.

I have a long-standing background in mineral exploration and research have been working on and off in this field since 1980. I have worked continuously in the business of mineral exploration since 2000.

I planned and worked with SkyTEM Canada Inc. regarding the airborne work conducted on the Que Property, May 25-26, 2020.

I have a direct interest in the Que Property, as I am the underlying owner of the property.

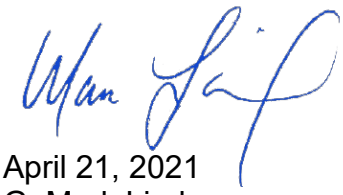

April 21, 2021
G. Mark Lindsay

LIST OF QUARTZ MINING CLAIMS

NAME	GRANT_#	TENURE	STATUS	OWNER	EXPIRY_DAT	DISTRICT
JOE 1	YC99823	Quartz	Active	Joanne McDougall - 50%; Nokuyukon Holdings Ltd. - 50%	3/7/2026	Whitehorse
JOE 2	YC99824	Quartz	Active	Joanne McDougall - 50%; Nokuyukon Holdings Ltd. - 50%	3/7/2026	Whitehorse
JOE 3	YC99825	Quartz	Active	Joanne McDougall - 50%; Nokuyukon Holdings Ltd. - 50%	3/7/2026	Whitehorse
JOE 4	YC99826	Quartz	Active	Joanne McDougall - 50%; Nokuyukon Holdings Ltd. - 50%	3/7/2026	Whitehorse
JOE 5	YC99827	Quartz	Active	Joanne McDougall - 50%; Nokuyukon Holdings Ltd. - 50%	3/7/2026	Whitehorse
JOE 6	YC99828	Quartz	Active	Joanne McDougall - 50%; Nokuyukon Holdings Ltd. - 50%	3/7/2026	Whitehorse
JOE 7	YC99829	Quartz	Active	Joanne McDougall - 50%; Nokuyukon Holdings Ltd. - 50%	3/7/2026	Whitehorse
JOE 8	YC99830	Quartz	Active	Joanne McDougall - 50%; Nokuyukon Holdings Ltd. - 50%	3/7/2026	Whitehorse
JOE 9	YC99831	Quartz	Active	Joanne McDougall - 50%; Nokuyukon Holdings Ltd. - 50%	3/7/2026	Whitehorse
JOE 10	YC99832	Quartz	Active	Joanne McDougall - 50%; Nokuyukon Holdings Ltd. - 50%	3/7/2026	Whitehorse
JOE 11	YC99833	Quartz	Active	Joanne McDougall - 50%; Nokuyukon Holdings Ltd. - 50%	3/7/2026	Whitehorse
JOE 12	YC99834	Quartz	Active	Joanne McDougall - 50%; Nokuyukon Holdings Ltd. - 50%	3/7/2026	Whitehorse
JOE 13	YC99835	Quartz	Active	Joanne McDougall - 50%; Nokuyukon Holdings Ltd. - 50%	3/7/2026	Whitehorse
JOE 14	YC99836	Quartz	Active	Joanne McDougall - 50%; Nokuyukon Holdings Ltd. - 50%	3/7/2026	Whitehorse
JOE 15	YC99837	Quartz	Active	Joanne McDougall - 50%; Nokuyukon Holdings Ltd. - 50%	3/7/2026	Whitehorse
JOE 16	YC99838	Quartz	Active	Joanne McDougall - 50%; Nokuyukon Holdings Ltd. - 50%	3/7/2026	Whitehorse
JOE 17	YC99839	Quartz	Active	Joanne McDougall - 50%; Nokuyukon Holdings Ltd. - 50%	3/7/2026	Whitehorse
JOE 18	YC99840	Quartz	Active	Joanne McDougall - 50%; Nokuyukon Holdings Ltd. - 50%	3/7/2026	Whitehorse
JOE 19	YC99841	Quartz	Active	Joanne McDougall - 50%; Nokuyukon Holdings Ltd. - 50%	3/7/2026	Whitehorse
JOE 20	YC99842	Quartz	Active	Joanne McDougall - 50%; Nokuyukon Holdings Ltd. - 50%	3/7/2026	Whitehorse
JOE 21	YC99843	Quartz	Active	Joanne McDougall - 50%; Nokuyukon Holdings Ltd. - 50%	3/7/2026	Whitehorse
JOE 22	YC99844	Quartz	Active	Joanne McDougall - 50%; Nokuyukon Holdings Ltd. - 50%	3/7/2026	Whitehorse
JOE 23	YC99845	Quartz	Active	Joanne McDougall - 50%; Nokuyukon Holdings Ltd. - 50%	3/7/2026	Whitehorse
JOE 24	YC99846	Quartz	Active	Joanne McDougall - 50%; Nokuyukon Holdings Ltd. - 50%	3/7/2026	Whitehorse
JOE 25	YC99847	Quartz	Active	Joanne McDougall - 50%; Nokuyukon Holdings Ltd. - 50%	3/7/2026	Whitehorse
JOE 26	YC99848	Quartz	Active	Joanne McDougall - 50%; Nokuyukon Holdings Ltd. - 50%	3/7/2026	Whitehorse
JOE 27	YC99849	Quartz	Active	Joanne McDougall - 50%; Nokuyukon Holdings Ltd. - 50%	3/7/2026	Whitehorse
JOE 28	YC99850	Quartz	Active	Joanne McDougall - 50%; Nokuyukon Holdings Ltd. - 50%	3/7/2026	Whitehorse
MIKLIN 99	YC26853	Quartz	Active	Mark Lindsay - 50%; Nokuyukon Holdings Ltd. - 50%	3/7/2026	Whitehorse
MIKLIN 101	YC26855	Quartz	Active	Mark Lindsay - 50%; Nokuyukon Holdings Ltd. - 50%	3/7/2026	Whitehorse
MIKLIN 103	YC26857	Quartz	Active	Mark Lindsay - 50%; Nokuyukon Holdings Ltd. - 50%	3/7/2026	Whitehorse
MIKLIN 105	YC26859	Quartz	Active	Mark Lindsay - 50%; Nokuyukon Holdings Ltd. - 50%	3/7/2026	Whitehorse
MIKLIN 107	YC26861	Quartz	Active	Mark Lindsay - 50%; Nokuyukon Holdings Ltd. - 50%	3/7/2026	Whitehorse
MIKLIN 109	YC26863	Quartz	Active	Mark Lindsay - 50%; Nokuyukon Holdings Ltd. - 50%	3/7/2026	Whitehorse
MIKLIN 111	YC26865	Quartz	Active	Mark Lindsay - 50%; Nokuyukon Holdings Ltd. - 50%	3/7/2026	Whitehorse
MIKLIN 131	YC26885	Quartz	Active	Mark Lindsay - 50%; Nokuyukon Holdings Ltd. - 50%	3/7/2026	Whitehorse
MIKLIN 132	YC26886	Quartz	Active	Mark Lindsay - 50%; Nokuyukon Holdings Ltd. - 50%	3/7/2026	Whitehorse
MIKLIN 133	YC26887	Quartz	Active	Mark Lindsay - 50%; Nokuyukon Holdings Ltd. - 50%	3/7/2026	Whitehorse
MIKLIN 134	YC26888	Quartz	Active	Mark Lindsay - 50%; Nokuyukon Holdings Ltd. - 50%	3/7/2026	Whitehorse
MIKLIN 135	YC26889	Quartz	Active	Mark Lindsay - 50%; Nokuyukon Holdings Ltd. - 50%	3/7/2026	Whitehorse
MIKLIN 136	YC26890	Quartz	Active	Mark Lindsay - 50%; Nokuyukon Holdings Ltd. - 50%	3/7/2026	Whitehorse
MIKLIN 137	YC26891	Quartz	Active	Mark Lindsay - 50%; Nokuyukon Holdings Ltd. - 50%	3/7/2026	Whitehorse
MIKLIN 138	YC26892	Quartz	Active	Mark Lindsay - 50%; Nokuyukon Holdings Ltd. - 50%	3/7/2026	Whitehorse
MIKLIN 139	YC26893	Quartz	Active	Mark Lindsay - 50%; Nokuyukon Holdings Ltd. - 50%	3/7/2026	Whitehorse
MIKLIN 140	YC26894	Quartz	Active	Mark Lindsay - 50%; Nokuyukon Holdings Ltd. - 50%	3/7/2026	Whitehorse
MIKLIN 141	YC26895	Quartz	Active	Mark Lindsay - 50%; Nokuyukon Holdings Ltd. - 50%	3/7/2026	Whitehorse
MIKLIN 142	YC26896	Quartz	Active	Mark Lindsay - 50%; Nokuyukon Holdings Ltd. - 50%	3/7/2026	Whitehorse
MIKLIN 143	YC26897	Quartz	Active	Mark Lindsay - 50%; Nokuyukon Holdings Ltd. - 50%	3/7/2026	Whitehorse
MIKLIN 144	YC26898	Quartz	Active	Mark Lindsay - 50%; Nokuyukon Holdings Ltd. - 50%	3/7/2026	Whitehorse
MIKLIN 145	YC26899	Quartz	Active	Mark Lindsay - 50%; Nokuyukon Holdings Ltd. - 50%	3/7/2026	Whitehorse

NAME	GRANT_#	TENURE	STATUS	OWNER	EXPIRY_DAT	DISTRICT
MIKLIN 146	YC26900	Quartz	Active	Mark Lindsay - 50%; Nokuyukon Holdings Ltd. - 50%	3/7/2026	Whitehorse
MIKLIN 147	YC29801	Quartz	Active	Mark Lindsay - 50%; Nokuyukon Holdings Ltd. - 50%	3/7/2026	Whitehorse
MIKLIN 148	YC29802	Quartz	Active	Mark Lindsay - 50%; Nokuyukon Holdings Ltd. - 50%	3/7/2026	Whitehorse
MIKLIN 163	YC29817	Quartz	Active	Mark Lindsay - 50%; Nokuyukon Holdings Ltd. - 50%	3/7/2026	Whitehorse
MIKLIN 164	YC29818	Quartz	Active	Mark Lindsay - 50%; Nokuyukon Holdings Ltd. - 50%	3/7/2026	Whitehorse
MIKLIN 165	YC29819	Quartz	Active	Mark Lindsay - 50%; Nokuyukon Holdings Ltd. - 50%	3/7/2026	Whitehorse
MIKLIN 166	YC29820	Quartz	Active	Mark Lindsay - 50%; Nokuyukon Holdings Ltd. - 50%	3/7/2026	Whitehorse
MIKLIN 167	YC29821	Quartz	Active	Mark Lindsay - 50%; Nokuyukon Holdings Ltd. - 50%	3/7/2026	Whitehorse
MIKLIN 168	YC29822	Quartz	Active	Mark Lindsay - 50%; Nokuyukon Holdings Ltd. - 50%	3/7/2026	Whitehorse
MIKLIN 169	YC29823	Quartz	Active	Mark Lindsay - 50%; Nokuyukon Holdings Ltd. - 50%	3/7/2026	Whitehorse
MIKLIN 170	YC29824	Quartz	Active	Mark Lindsay - 50%; Nokuyukon Holdings Ltd. - 50%	3/7/2026	Whitehorse
MIKLIN 171	YC29825	Quartz	Active	Mark Lindsay - 50%; Nokuyukon Holdings Ltd. - 50%	3/7/2026	Whitehorse
MIKLIN 172	YC29826	Quartz	Active	Mark Lindsay - 50%; Nokuyukon Holdings Ltd. - 50%	3/7/2026	Whitehorse
MIKLIN 173	YC29827	Quartz	Active	Mark Lindsay - 50%; Nokuyukon Holdings Ltd. - 50%	3/7/2026	Whitehorse
MIKLIN 174	YC29828	Quartz	Active	Mark Lindsay - 50%; Nokuyukon Holdings Ltd. - 50%	3/7/2026	Whitehorse
MIKLIN 175	YC29829	Quartz	Active	Mark Lindsay - 50%; Nokuyukon Holdings Ltd. - 50%	3/7/2026	Whitehorse
MIKLIN 176	YC29830	Quartz	Active	Mark Lindsay - 50%; Nokuyukon Holdings Ltd. - 50%	3/7/2026	Whitehorse
MIKLIN 177	YC29831	Quartz	Active	Mark Lindsay - 50%; Nokuyukon Holdings Ltd. - 50%	3/7/2026	Whitehorse
MIKLIN 178	YC29832	Quartz	Active	Mark Lindsay - 50%; Nokuyukon Holdings Ltd. - 50%	3/7/2026	Whitehorse
MIKLIN 179	YC29833	Quartz	Active	Mark Lindsay - 50%; Nokuyukon Holdings Ltd. - 50%	3/7/2026	Whitehorse
MIKLIN 180	YC29834	Quartz	Active	Mark Lindsay - 50%; Nokuyukon Holdings Ltd. - 50%	3/7/2026	Whitehorse
MIKLIN 196	YC29850	Quartz	Active	Mark Lindsay - 50%; Nokuyukon Holdings Ltd. - 50%	3/7/2026	Whitehorse
MIKLIN 198	YC29852	Quartz	Active	Mark Lindsay - 50%; Nokuyukon Holdings Ltd. - 50%	3/7/2026	Whitehorse
MIKLIN 200	YC29854	Quartz	Active	Mark Lindsay - 50%; Nokuyukon Holdings Ltd. - 50%	3/7/2026	Whitehorse
MIKLIN 202	YC29856	Quartz	Active	Mark Lindsay - 50%; Nokuyukon Holdings Ltd. - 50%	3/7/2026	Whitehorse
MIKLIN 204	YC29858	Quartz	Active	Mark Lindsay - 50%; Nokuyukon Holdings Ltd. - 50%	3/7/2026	Whitehorse
MIKLIN 206	YC29860	Quartz	Active	Mark Lindsay - 50%; Nokuyukon Holdings Ltd. - 50%	3/7/2026	Whitehorse
MIKLIN 208	YC29862	Quartz	Active	Mark Lindsay - 50%; Nokuyukon Holdings Ltd. - 50%	3/7/2026	Whitehorse
MIKLIN 210	YC29864	Quartz	Active	Mark Lindsay - 50%; Nokuyukon Holdings Ltd. - 50%	3/7/2026	Whitehorse
MIKLIN 212	YC29866	Quartz	Active	Mark Lindsay - 50%; Nokuyukon Holdings Ltd. - 50%	3/7/2026	Whitehorse
QUE 1	YF75901	Quartz	Active	Stuhini Exploration Ltd. - 100%	3/7/2026	Whitehorse
QUE 2	YF75902	Quartz	Active	Stuhini Exploration Ltd. - 100%	3/7/2026	Whitehorse
QUE 3	YF75903	Quartz	Active	Stuhini Exploration Ltd. - 100%	3/7/2026	Whitehorse
QUE 4	YF75904	Quartz	Active	Stuhini Exploration Ltd. - 100%	3/7/2026	Whitehorse
QUE 5	YF75905	Quartz	Active	Stuhini Exploration Ltd. - 100%	3/7/2026	Whitehorse
QUE 6	YF75906	Quartz	Active	Stuhini Exploration Ltd. - 100%	3/7/2026	Whitehorse
QUE 7	YF75907	Quartz	Active	Stuhini Exploration Ltd. - 100%	3/7/2026	Whitehorse
QUE 8	YF75908	Quartz	Active	Stuhini Exploration Ltd. - 100%	3/7/2026	Whitehorse
QUE 9	YF75909	Quartz	Active	Stuhini Exploration Ltd. - 100%	3/7/2026	Whitehorse
QUE 10	YF75910	Quartz	Active	Stuhini Exploration Ltd. - 100%	3/7/2026	Whitehorse
QUE 11	YF75911	Quartz	Active	Stuhini Exploration Ltd. - 100%	3/7/2026	Whitehorse
QUE 12	YF75912	Quartz	Active	Stuhini Exploration Ltd. - 100%	3/7/2026	Whitehorse
QUE 13	YF75913	Quartz	Active	Stuhini Exploration Ltd. - 100%	3/7/2026	Whitehorse
QUE 14	YF75914	Quartz	Active	Stuhini Exploration Ltd. - 100%	3/7/2026	Whitehorse
QUE 15	YF75915	Quartz	Active	Stuhini Exploration Ltd. - 100%	3/7/2026	Whitehorse
QUE 16	YF75916	Quartz	Active	Stuhini Exploration Ltd. - 100%	3/7/2026	Whitehorse
QUE 17	YF75917	Quartz	Active	Stuhini Exploration Ltd. - 100%	3/7/2026	Whitehorse
QUE 18	YF75918	Quartz	Active	Stuhini Exploration Ltd. - 100%	3/7/2026	Whitehorse
QUE 19	YF75919	Quartz	Active	Stuhini Exploration Ltd. - 100%	3/7/2026	Whitehorse
QUE 20	YF75920	Quartz	Active	Stuhini Exploration Ltd. - 100%	3/7/2026	Whitehorse
QUE 21	YF75921	Quartz	Active	Stuhini Exploration Ltd. - 100%	3/7/2026	Whitehorse
QUE 22	YF75922	Quartz	Active	Stuhini Exploration Ltd. - 100%	3/7/2026	Whitehorse
QUE 23	YF75923	Quartz	Active	Stuhini Exploration Ltd. - 100%	3/7/2026	Whitehorse
QUE 24	YF75924	Quartz	Active	Stuhini Exploration Ltd. - 100%	3/7/2026	Whitehorse
QUE 25	YF75925	Quartz	Active	Stuhini Exploration Ltd. - 100%	3/7/2026	Whitehorse

NAME	GRANT_#	TENURE	STATUS	OWNER	EXPIRY_DAT	DISTRICT
QUE 26	YF75926	Quartz	Active	Stuhini Exploration Ltd. - 100%	3/7/2026	Whitehorse
QUE 27	YF75927	Quartz	Active	Stuhini Exploration Ltd. - 100%	3/7/2026	Whitehorse
QUE 28	YF75928	Quartz	Active	Stuhini Exploration Ltd. - 100%	3/7/2026	Whitehorse
QUE 29	YF75929	Quartz	Active	Stuhini Exploration Ltd. - 100%	3/7/2026	Whitehorse
QUE 30	YF75930	Quartz	Active	Stuhini Exploration Ltd. - 100%	3/7/2026	Whitehorse
QUE 31	YF75931	Quartz	Active	Stuhini Exploration Ltd. - 100%	3/7/2026	Whitehorse
QUE 32	YF75932	Quartz	Active	Stuhini Exploration Ltd. - 100%	3/7/2026	Whitehorse
QUE 33	YF75933	Quartz	Active	Stuhini Exploration Ltd. - 100%	3/7/2026	Whitehorse
QUE 34	YF75934	Quartz	Active	Stuhini Exploration Ltd. - 100%	3/7/2026	Whitehorse
QUE 35	YF75935	Quartz	Active	Stuhini Exploration Ltd. - 100%	3/7/2026	Whitehorse
QUE 36	YF75936	Quartz	Active	Stuhini Exploration Ltd. - 100%	3/7/2026	Whitehorse
QUE 37	YF75937	Quartz	Active	Stuhini Exploration Ltd. - 100%	3/7/2026	Whitehorse
QUE 38	YF75938	Quartz	Active	Stuhini Exploration Ltd. - 100%	3/7/2026	Whitehorse
QUE 39	YF75939	Quartz	Active	Stuhini Exploration Ltd. - 100%	3/7/2026	Whitehorse
QUE 40	YF75940	Quartz	Active	Stuhini Exploration Ltd. - 100%	3/7/2026	Whitehorse
QUE 41	YF75941	Quartz	Active	Stuhini Exploration Ltd. - 100%	3/7/2026	Whitehorse
QUE 42	YF75942	Quartz	Active	Stuhini Exploration Ltd. - 100%	3/7/2026	Whitehorse
QUE 43	YF75943	Quartz	Active	Stuhini Exploration Ltd. - 100%	3/7/2026	Whitehorse
QUE 44	YF75944	Quartz	Active	Stuhini Exploration Ltd. - 100%	3/7/2026	Whitehorse
QUE 45	YF75945	Quartz	Active	Stuhini Exploration Ltd. - 100%	3/7/2026	Whitehorse
QUE 46	YF75946	Quartz	Active	Stuhini Exploration Ltd. - 100%	3/7/2026	Whitehorse
QUE 47	YF75947	Quartz	Active	Stuhini Exploration Ltd. - 100%	3/7/2026	Whitehorse
QUE 48	YF75948	Quartz	Active	Stuhini Exploration Ltd. - 100%	3/7/2026	Whitehorse
QUE 49	YF75949	Quartz	Active	Stuhini Exploration Ltd. - 100%	3/7/2026	Whitehorse
QUE 50	YF75950	Quartz	Active	Stuhini Exploration Ltd. - 100%	3/7/2026	Whitehorse
QUE 51	YF75951	Quartz	Active	Stuhini Exploration Ltd. - 100%	3/7/2026	Whitehorse
QUE 52	YF75952	Quartz	Active	Stuhini Exploration Ltd. - 100%	3/7/2026	Whitehorse
QUE 53	YF75953	Quartz	Active	Stuhini Exploration Ltd. - 100%	3/7/2026	Whitehorse
QUE 54	YF75954	Quartz	Active	Stuhini Exploration Ltd. - 100%	3/7/2026	Whitehorse
QUE 55	YF75955	Quartz	Active	Stuhini Exploration Ltd. - 100%	3/7/2026	Whitehorse
QUE 56	YF75956	Quartz	Active	Stuhini Exploration Ltd. - 100%	3/7/2026	Whitehorse
QUE 57	YF75957	Quartz	Active	Stuhini Exploration Ltd. - 100%	3/7/2026	Whitehorse
QUE 58	YF75958	Quartz	Active	Stuhini Exploration Ltd. - 100%	3/7/2026	Whitehorse
QUE 59	YF75959	Quartz	Active	Stuhini Exploration Ltd. - 100%	3/7/2026	Whitehorse
QUE 60	YF75960	Quartz	Active	Stuhini Exploration Ltd. - 100%	3/7/2026	Whitehorse
QUE 61	YF75961	Quartz	Active	Stuhini Exploration Ltd. - 100%	3/7/2026	Whitehorse
QUE 62	YF75962	Quartz	Active	Stuhini Exploration Ltd. - 100%	3/7/2026	Whitehorse
QUE 63	YF75963	Quartz	Active	Stuhini Exploration Ltd. - 100%	3/7/2026	Whitehorse
QUE 64	YF75964	Quartz	Active	Stuhini Exploration Ltd. - 100%	3/7/2026	Whitehorse
QUE 65	YF75965	Quartz	Active	Stuhini Exploration Ltd. - 100%	3/7/2026	Whitehorse
QUE 66	YF75966	Quartz	Active	Stuhini Exploration Ltd. - 100%	3/7/2026	Whitehorse
QUE 67	YF75967	Quartz	Active	Stuhini Exploration Ltd. - 100%	3/7/2026	Whitehorse
QUE 68	YF75968	Quartz	Active	Stuhini Exploration Ltd. - 100%	3/7/2026	Whitehorse
QUE 69	YF75969	Quartz	Active	Stuhini Exploration Ltd. - 100%	3/7/2026	Whitehorse
QUE 70	YF75970	Quartz	Active	Stuhini Exploration Ltd. - 100%	3/7/2026	Whitehorse
QUE 71	YF75971	Quartz	Active	Stuhini Exploration Ltd. - 100%	3/7/2026	Whitehorse
QUE 72	YF75972	Quartz	Active	Stuhini Exploration Ltd. - 100%	3/7/2026	Whitehorse
QUE 73	YF75973	Quartz	Active	Stuhini Exploration Ltd. - 100%	3/7/2026	Whitehorse
QUE 74	YF75974	Quartz	Active	Stuhini Exploration Ltd. - 100%	3/7/2026	Whitehorse
QUE 75	YF75975	Quartz	Active	Stuhini Exploration Ltd. - 100%	3/7/2026	Whitehorse
QUE 76	YF75976	Quartz	Active	Stuhini Exploration Ltd. - 100%	3/7/2026	Whitehorse
QUE 77	YF75977	Quartz	Active	Stuhini Exploration Ltd. - 100%	3/7/2026	Whitehorse
QUE 78	YF75978	Quartz	Active	Stuhini Exploration Ltd. - 100%	3/7/2026	Whitehorse
QUE 79	YF75979	Quartz	Active	Stuhini Exploration Ltd. - 100%	3/7/2026	Whitehorse
QUE 80	YF75980	Quartz	Active	Stuhini Exploration Ltd. - 100%	3/7/2026	Whitehorse

NAME	GRANT_#	TENURE	STATUS	OWNER	EXPIRY_DAT	DISTRICT
QUE 81	YF75981	Quartz	Active	Stuhini Exploration Ltd. - 100%	3/7/2026	Whitehorse
QUE 82	YF75982	Quartz	Active	Stuhini Exploration Ltd. - 100%	3/7/2026	Whitehorse
QUE 83	YF75983	Quartz	Active	Stuhini Exploration Ltd. - 100%	3/7/2026	Whitehorse
QUE 84	YF75984	Quartz	Active	Stuhini Exploration Ltd. - 100%	3/7/2026	Whitehorse
QUE 85	YF75985	Quartz	Active	Stuhini Exploration Ltd. - 100%	3/7/2026	Whitehorse
QUE 86	YF75986	Quartz	Active	Stuhini Exploration Ltd. - 100%	3/7/2026	Whitehorse
QUE 87	YF75987	Quartz	Active	Stuhini Exploration Ltd. - 100%	3/7/2026	Whitehorse
QUE 88	YF75988	Quartz	Active	Stuhini Exploration Ltd. - 100%	3/7/2026	Whitehorse
QUE 89	YF75989	Quartz	Active	Stuhini Exploration Ltd. - 100%	3/7/2026	Whitehorse
QUE 90	YF75990	Quartz	Active	Stuhini Exploration Ltd. - 100%	3/7/2026	Whitehorse
QUE 91	YF75991	Quartz	Active	Stuhini Exploration Ltd. - 100%	3/7/2026	Whitehorse
QUE 92	YF75992	Quartz	Active	Stuhini Exploration Ltd. - 100%	3/7/2026	Whitehorse
QUE 93	YF75993	Quartz	Active	Stuhini Exploration Ltd. - 100%	3/7/2026	Whitehorse
QUE 94	YF75994	Quartz	Active	Stuhini Exploration Ltd. - 100%	3/7/2026	Whitehorse
QUE 95	YF75995	Quartz	Active	Stuhini Exploration Ltd. - 100%	3/7/2026	Whitehorse
QUE 96	YF75996	Quartz	Active	Stuhini Exploration Ltd. - 100%	3/7/2026	Whitehorse
TCR 1	YD35457	Quartz	Active	Nokuyukon Holdings Ltd. - 100%	3/7/2026	Whitehorse
TCR 2	YD35458	Quartz	Active	Nokuyukon Holdings Ltd. - 100%	3/7/2026	Whitehorse
TCR 3	YD35459	Quartz	Active	Nokuyukon Holdings Ltd. - 100%	3/7/2026	Whitehorse
TCR 4	YD35460	Quartz	Active	Nokuyukon Holdings Ltd. - 100%	3/7/2026	Whitehorse
TCR 5	YD35461	Quartz	Active	Nokuyukon Holdings Ltd. - 100%	3/7/2026	Whitehorse
TCR 6	YD35462	Quartz	Active	Nokuyukon Holdings Ltd. - 100%	3/7/2026	Whitehorse
TCR 7	YD35463	Quartz	Active	Nokuyukon Holdings Ltd. - 100%	3/7/2026	Whitehorse
TCR 8	YD35464	Quartz	Active	Nokuyukon Holdings Ltd. - 100%	3/7/2026	Whitehorse
TCR 9	YD35465	Quartz	Active	Nokuyukon Holdings Ltd. - 100%	3/7/2026	Whitehorse
TCR 10	YD35466	Quartz	Active	Nokuyukon Holdings Ltd. - 100%	3/7/2026	Whitehorse
TCR 11	YD35467	Quartz	Active	Nokuyukon Holdings Ltd. - 100%	3/7/2026	Whitehorse
TCR 12	YD35468	Quartz	Active	Nokuyukon Holdings Ltd. - 100%	3/7/2026	Whitehorse
TCR 13	YD35469	Quartz	Active	Nokuyukon Holdings Ltd. - 100%	3/7/2026	Whitehorse
TCR 14	YD35470	Quartz	Active	Nokuyukon Holdings Ltd. - 100%	3/7/2026	Whitehorse
TCR 15	YD35471	Quartz	Active	Nokuyukon Holdings Ltd. - 100%	3/7/2026	Whitehorse
TCR 16	YD35472	Quartz	Active	Nokuyukon Holdings Ltd. - 100%	3/7/2026	Whitehorse
TCR 17	YD35473	Quartz	Active	Nokuyukon Holdings Ltd. - 100%	3/7/2026	Whitehorse
TCR 18	YD35474	Quartz	Active	Nokuyukon Holdings Ltd. - 100%	3/7/2026	Whitehorse
TCR 19	YD35475	Quartz	Active	Nokuyukon Holdings Ltd. - 100%	3/7/2026	Whitehorse
TCR 20	YD35476	Quartz	Active	Nokuyukon Holdings Ltd. - 100%	3/7/2026	Whitehorse
TCR 21	YD118703	Quartz	Active	Nokuyukon Holdings Ltd. - 100%	3/7/2026	Whitehorse
TCR 22	YD118704	Quartz	Active	Nokuyukon Holdings Ltd. - 100%	3/7/2026	Whitehorse
TCR 23	YD118705	Quartz	Active	Nokuyukon Holdings Ltd. - 100%	3/7/2026	Whitehorse
TCR 24	YD118706	Quartz	Active	Nokuyukon Holdings Ltd. - 100%	3/7/2026	Whitehorse
TCR 25	YD118707	Quartz	Active	Nokuyukon Holdings Ltd. - 100%	3/7/2026	Whitehorse
TCR 26	YD118708	Quartz	Active	Nokuyukon Holdings Ltd. - 100%	3/7/2026	Whitehorse
TCR 27	YD118709	Quartz	Active	Nokuyukon Holdings Ltd. - 100%	3/7/2026	Whitehorse
TCR 28	YD118710	Quartz	Active	Nokuyukon Holdings Ltd. - 100%	3/7/2026	Whitehorse

APPENDIX 1 – AIRBORNE MAPS

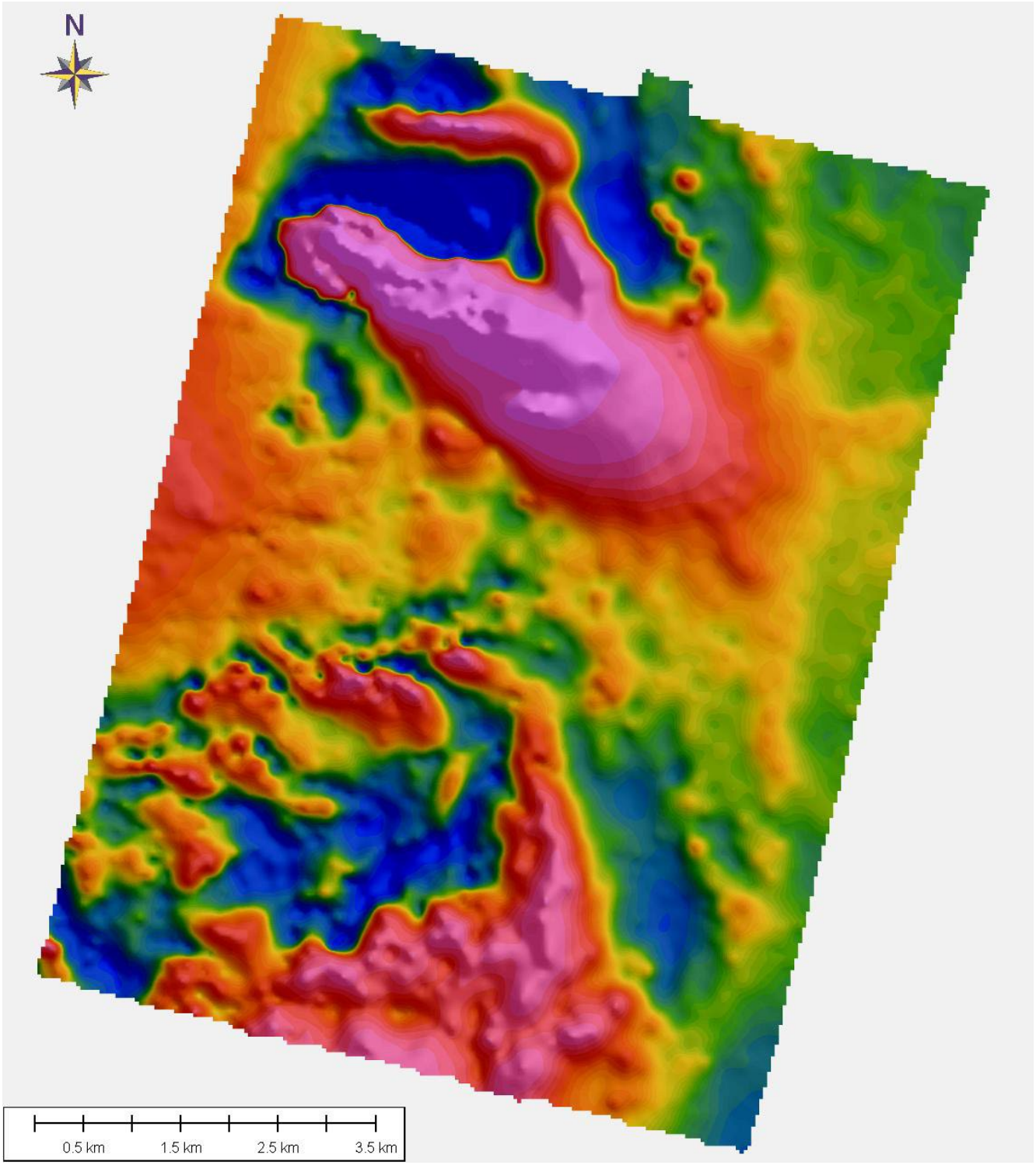

Figure 4 – TOTAL MAGNETIC IMAGE

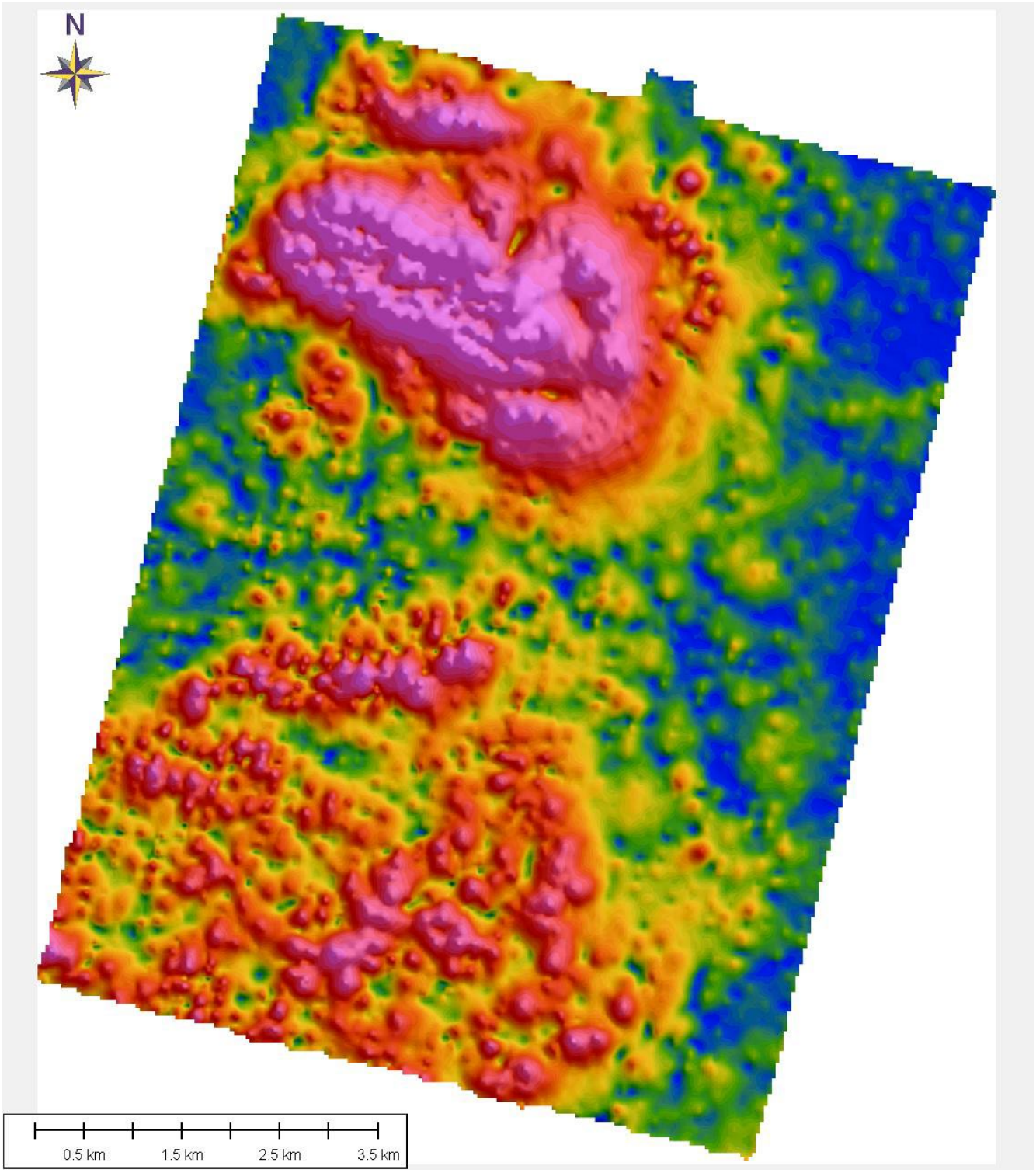

Figure 5 – ANALYTICAL SIGNAL MAGNETIC IMAGE

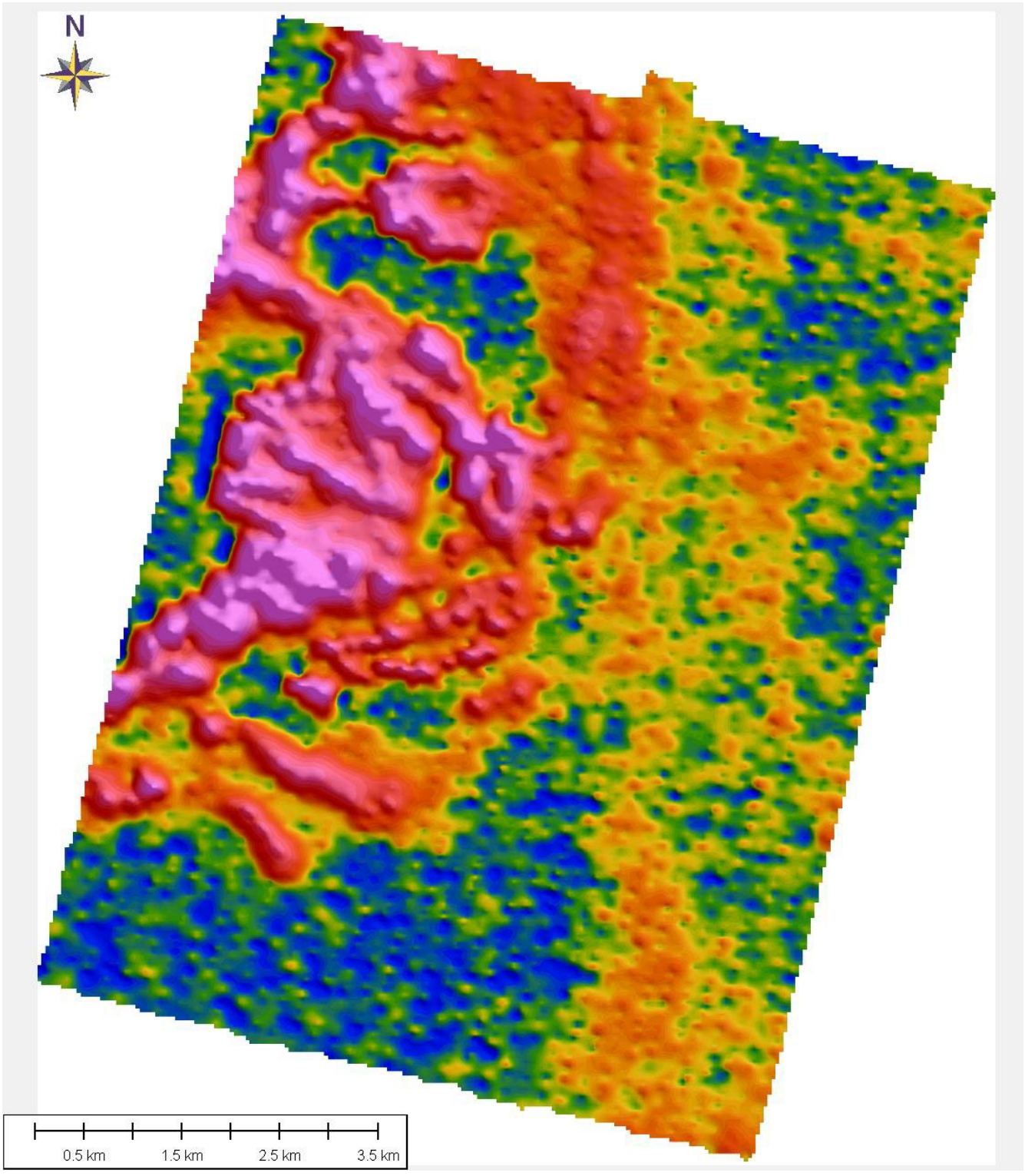

Figure 6 - QUE_air_TDEM_LM_Z[22]_40m_SkyTEM_2020 (Electromagnetic Anomalies)

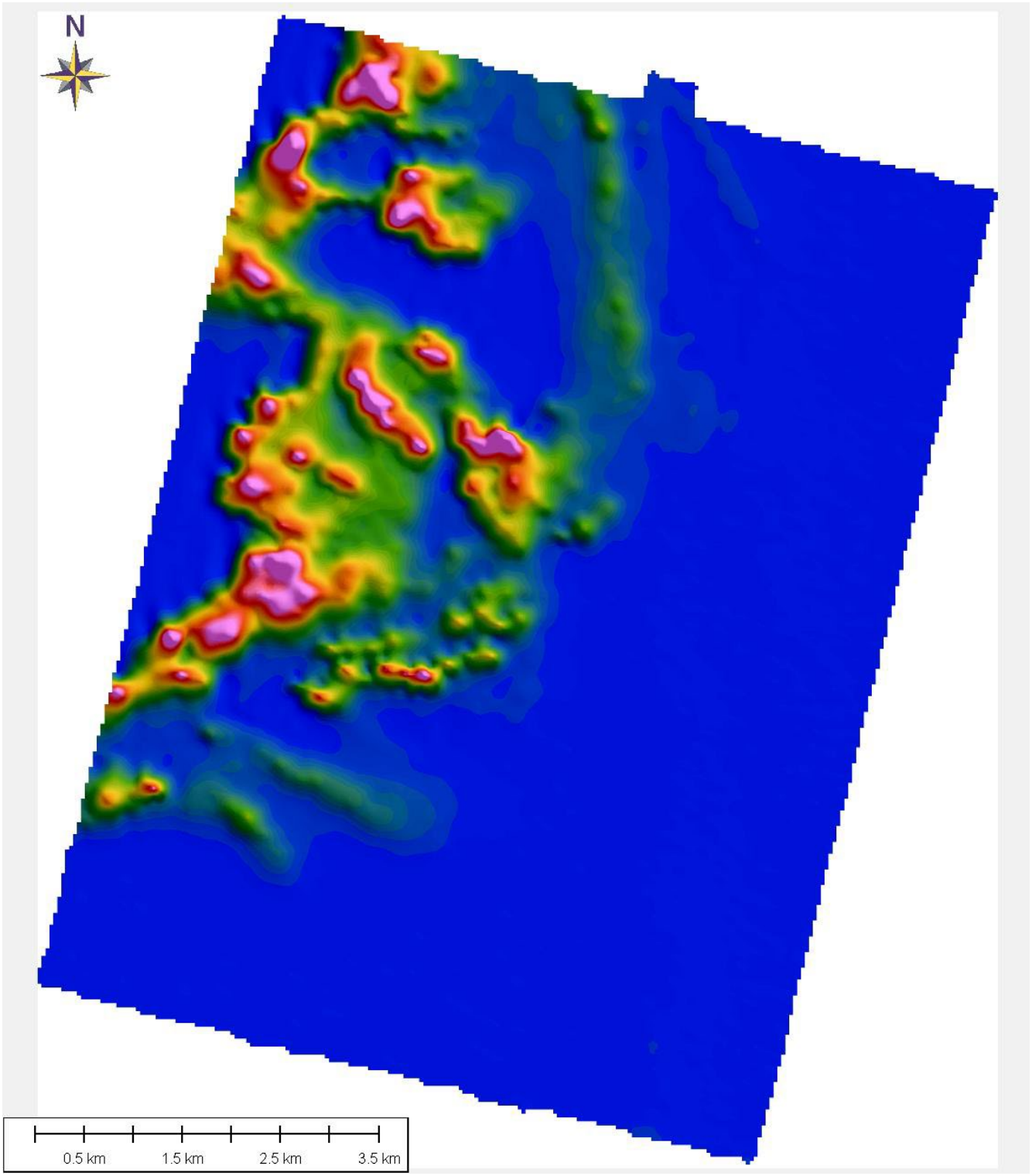

Figure 7 - QUE_air_TDEM_HM_Z[24]_40m_SkyTEM_2020 (Electromagnetic Anomalies)

DATA REPORT

SkyTEM Survey:

Que Block SkyTEM312M,
Johnson Crossing, Yukon

Client: Stuhini Exploration Ltd.

Date: July 2020

SKYTEM AIRBORNE SURVEYS WORLDWIDE

SKYTEM SURVEYS APS
DYSSEN 2
8200 AARHUS N, DENMARK

TEL: +45 8620 2050
VAT: 27704379

WWW.SKYTEM.COM
INFO@SKYTEM.COM

Structure of the Digital Data Delivery catalogue

Folder	Sub folder	Sub folder	File format	Content
01_Data			.gdb	Survey Data
02_Inversion	01_GDB_Models		.gdb	Modelled layer conductivity database
	02_Layer_conductivity_Grids	01_GS_Grd 02_GeoTiff	.grd .tif	Modelled layer conductivity grids
	03_Layer_conductivity_Maps		.map	Modelled layer conductivity maps
	04_Sections		.png	Profile sections of modelled layer conductivity & model analysis
03_Maps	01_DEM			DEM
	02_Linepath			Flown Flight lines and Planned Flight Lines
	03_MAG			Magnetic data
	04_EM_HMZ_HCorr			Height Corrected EM data
	05_EM_LMZ_HCorr			
04_Grids	01_DEM		.grd	Digital Elevation Model
	02_EM	01_HM_Z	.grd	Height Corrected EM grids
		02_LM_Z		
	03_MAG		.grd .png	Total Magnetic Intensity and Residual Magnetic Field
05_Report				Data report

Contents

Executive Summary

This report covers data acquisition, technical specifications, data processing and presentation of the SkyTEM 312M survey flown on May 25th, and 26th, 2020 over the Que Block, Yukon. The survey is comprised of one block with 425 km planned flight lines in total.

The SkyTEM 312M collects time domain electromagnetic and magnetic data along with supporting navigation measurements.

All material is delivered digitally. The final product includes:

- Data report
- Processed data as Geosoft database file format
- Inversion results; modelled layer conductivity in Geosoft database file format
- Grids and maps in Geosoft format
- Presentations of data and inversion results in png and Geotiff format

An overview of the digital data delivery can be seen on the front inside cover of this report.

Introduction

The SkyTEM electromagnetic and magnetic survey described in this report was flown with the SkyTEM 312M system. The survey is requested by Stuhini Exploration Ltd. and performed by SkyTEM Canada Inc. Basic survey information and key personnel are listed in Table 1.

This report covers data acquisition, instrument descriptions, data processing and presentations. The data delivery includes processed magnetic and electromagnetic data and presentations, spatially constrained inversion results and model presentations. The digital data delivery folder is described in the front inside cover of this report.

This report does not include any geological interpretations of the geophysical dataset.

Stuhini Exploration Ltd. (Client) Client Contact person	 Dave O'Brien Email: dobrien@stuhini.com
SkyTEM Canada Inc (Contractor) Contact person Project Manager Field Crew	 Gary Tipper Email: gti@skytem.com Doug Garrie P.Geo Email: dga@skytem.com David Nauss Nicholas Boucher
Great Slave Helicopters (Helicopter operator) Helicopter type Pilot	 Eurocopter Astar 350 B3 Kevin Duff
Data acquisition period	May 25th, and 26th, 2020
Data processing, presentations and report	Doug Garrie P.Geo

Table 1 Key personnel and survey information.

Survey outline

The survey area is located near of Johnson Crossing, Yukon and was flown on May 25th, and 26th, 2020.

Planned l-km are listed in Table 2, and actual flown line-km are listed in Table 3. Line numbering is listed in Table 4.

Actual flown lines (red lines) versus planned lines (blue lines) are presented on Figure 1 and Figure 2.

Discrepancies between planned and flown lines occur where obstacles on the ground or weather necessitates a diversion.

Tie lines were flown perpendicular to the transverse lines.

The coordinate system is kept in UTM Zone 8N (WGS84) throughout this report and the digital data delivery.

Area name	Traverse spacing (m)	Traverse direction (deg)	Tie line spacing (m)	Flight lines (km)	Tie lines (km)	Total line kilometers (km)
Que Block	200	14°/194°	2000	381.0	44	**425 km**

Table 2 Planned Survey details

Area name	Flight lines (km)	Tie lines (km)	Total line kilometers (km)
Que Block	385.9	45.7	**431.6 km**

Table 3 Actual L-Km flown

Area	Line numbering	Tie line numbering
Que Block	L100101 – L103801	L200101 – L200701

Table 4 Line numbering

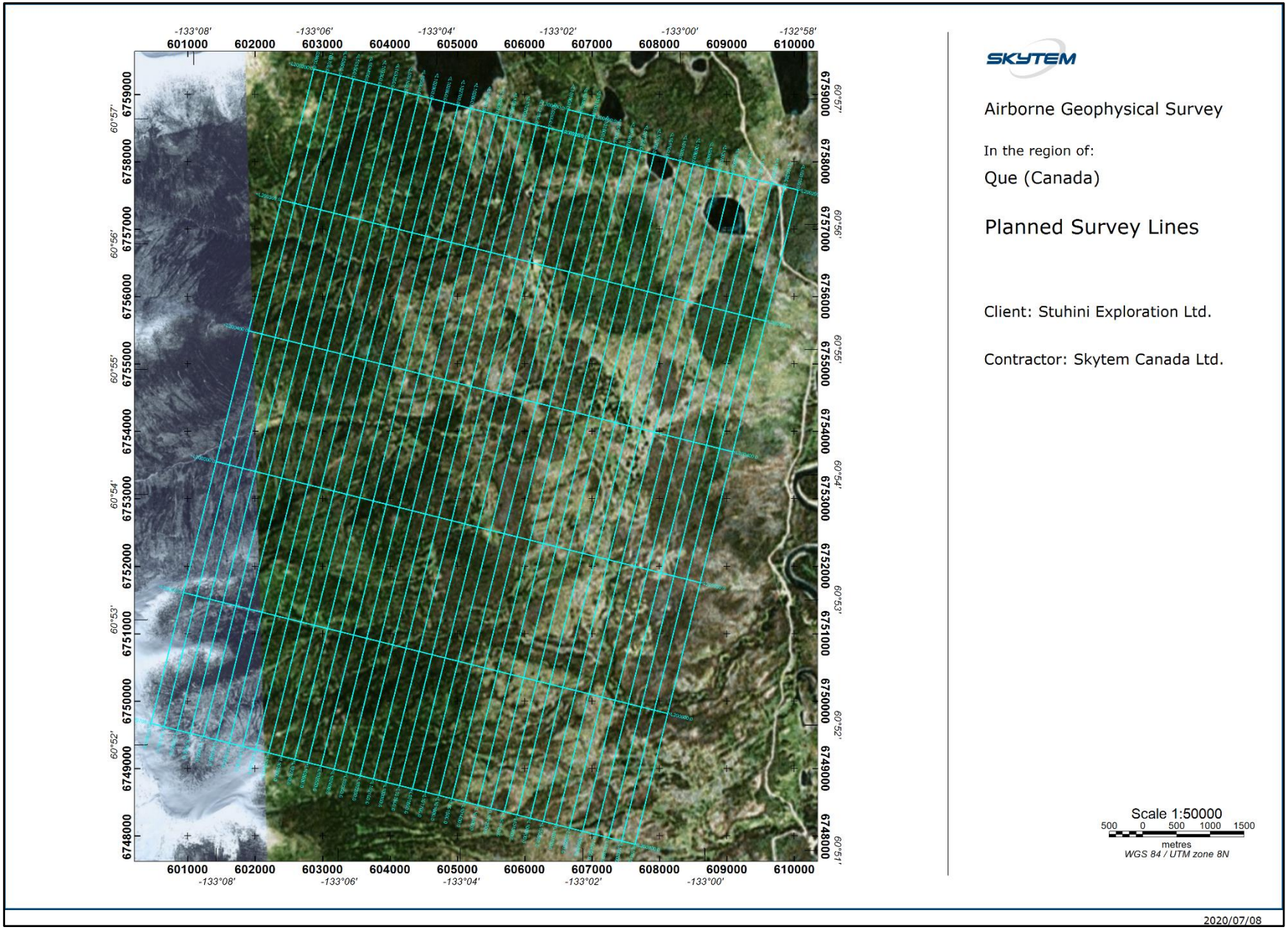

Figure 1. Survey outline. Blue lines represent the planned survey lines.

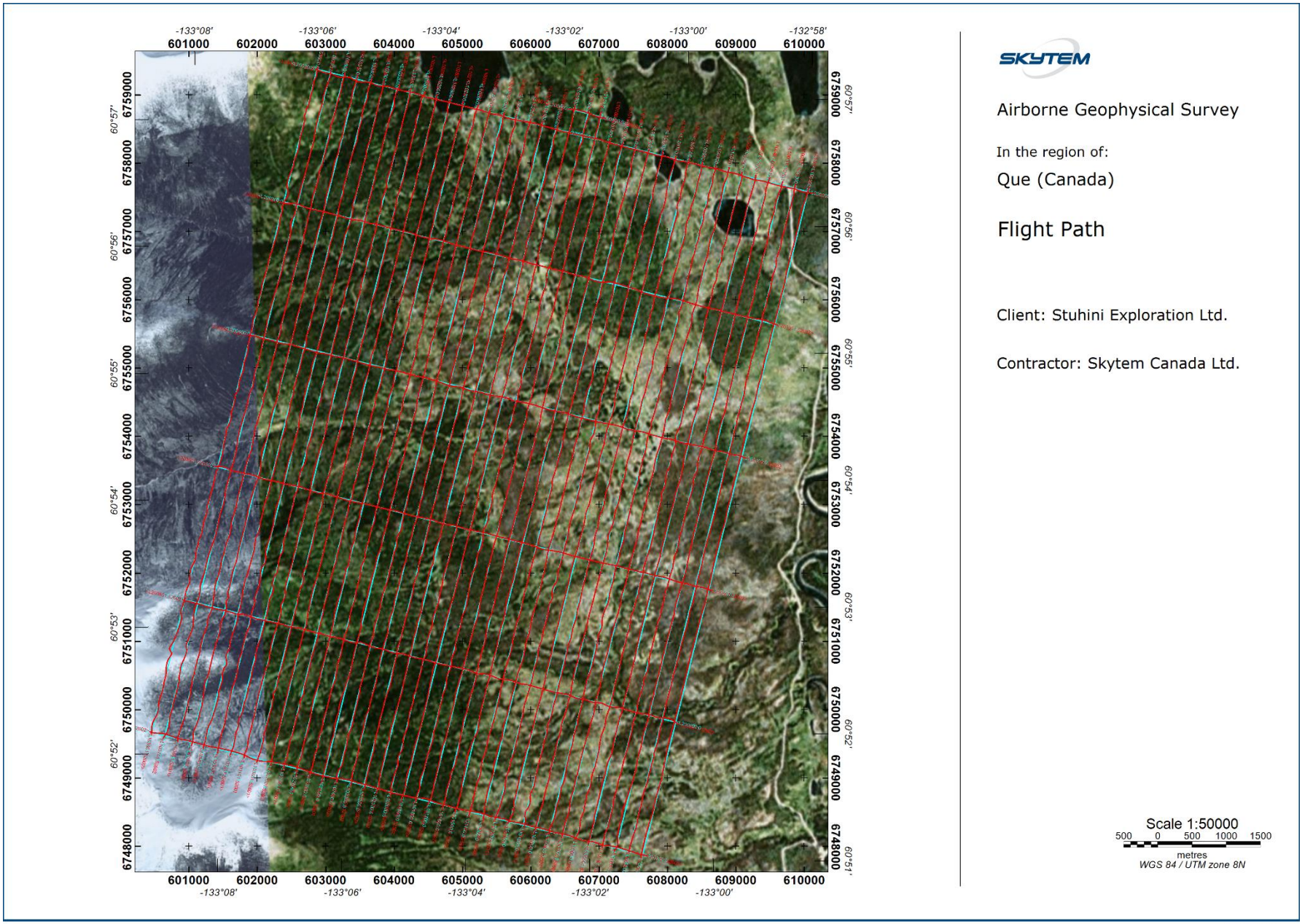

Figure 2. Flown lines (red) superimposed on planned lines (blue).

Flight Parameters

The nominal terrain clearance is 50 m, with an increase due to steep terrain, forests, power lines, or any other obstacles or hazards on the ground. The safe flying height during the survey is always based on the pilot's assessment of risk and deviations from nominal values are at the discretion of the pilot.

The nominal production airspeed is 60 - 110 kph for a flat topography with no wind. This may vary in areas of rugged terrain and/or windy conditions.

Average values and standard deviations of survey flight parameters are found in Table 5:

Control parameter		Average Value	Standard Deviation
Ground speed*)		71.4 kph	11.4 kph
Processed height		45.9 m	7.9 m
Tilt angle	X	-2.5 degrees	2.86 degrees
	Y	2.0 degrees	1.3 degrees
Tx Voltage	Tx_off	71.270.2 V	-
	Tx_on	65.965.9 V	-
Low Monent Current		5.9 A	0.01 A
High Moment Current		110.5 A	2.4 A
Tx temperature		~23 23°C	-

**) Actual speed varies as a function of day and flight direction due to different wind directions and magnitude.*

Table 5 Flight parameters for the area

Flight Reports

For each flight, a report with key information regarding the data acquisition is made in the field. Listed in the reports are details on the weather, special data parameters and other events which may influence data. Selected information from the flight reports are shown in Table 6 and Table 7.

Flight	Comments
20200525.01	Production Flight #1
20200525.03	Production Flight #2
20200526.01	Production Flight #3
20200526.02	Production Flight #4
20200527.01	Ferry JC to Atlin
20200528.01	Production Flight #5
20200528.02	Production Flight #6
20200529.01	Production Flight #7
20200529.02	Production Flight #8
20200531.01	Production Flight #9
20200601.01	Production Flight #10
20200601.02	Production Flight #11
20200602.01	Production Flight #12
20200602.02	Production Flight #13
20200603.01	Production Flight #14
20200603.02	Production Flight #15
20200603.03	Production Flight #16
20200604.01	Production Flight #17
20200604.02	Production Flight #18
20200604.03	Production Flight #19

Table 6. Flight report

Flight	Temperature (C)	Wind (m/s)	Visibility	Description
20200523.01	10		Great	clear skies
20200523.02	13		Great	clear skies
20200523.03	16		Great	few clouds
20200525.01	3	3 to 4 North	Great	Covered
20200525.02	6		Great	Covered
20200525.03	8	6 to 10 North	Great	Covered
20200526.01	3			Covered
20200526.02	9			Covered
20200527.01				

20200528.01	8	9 to 12 W	Great	Few clouds
20200528.02	10	12 to 18 W	good	Covered
20200529.01	6	9 to 12 W	ok	Covered Light showers on the ferry
20200529.02	9	10 to 16 W	ok	Covered
20200531.01	8	8 to14 W	ok	Covered
20200601.01	8	9 to 15 W	ok	Covered
20200601.02	10	10 to 16 W	ok	Covered
20200602.01	6		ok	Covered
20200602.02	9		ok	Covered
20200603.01	6		ok	scattered
20200603.02	10		ok	scattered
20200603.03	13		ok	scattered
20200604.01	6		ok	scattered
20200604.02	8		ok	scattered
20200604.03	12		ok	scattered

Table 7. Weather report

Instruments

This section provides an overview of airborne as well as ground base instruments, thorough technical descriptions are provided in Appendix 1.

Airborne unit

The airborne instrumentation comprising a SkyTEM 312M system includes a time domain electromagnetic system, a magnetic data acquisition system and an auxiliary data acquisition system containing two inclinometers, two altimeters and two DGPS'. All instruments are mounted on the frame suspended ~40 m below the helicopter. The generator used to power the transmitter is suspended between the frame and the helicopter about 30 m below the helicopter. A picture of the airborne SkyTEM 312M unit is seen on Figure 3, and a sketch of the instrumentation is seen on Figure 4.

Figure 3 SkyTEM 312M Airborne unit.

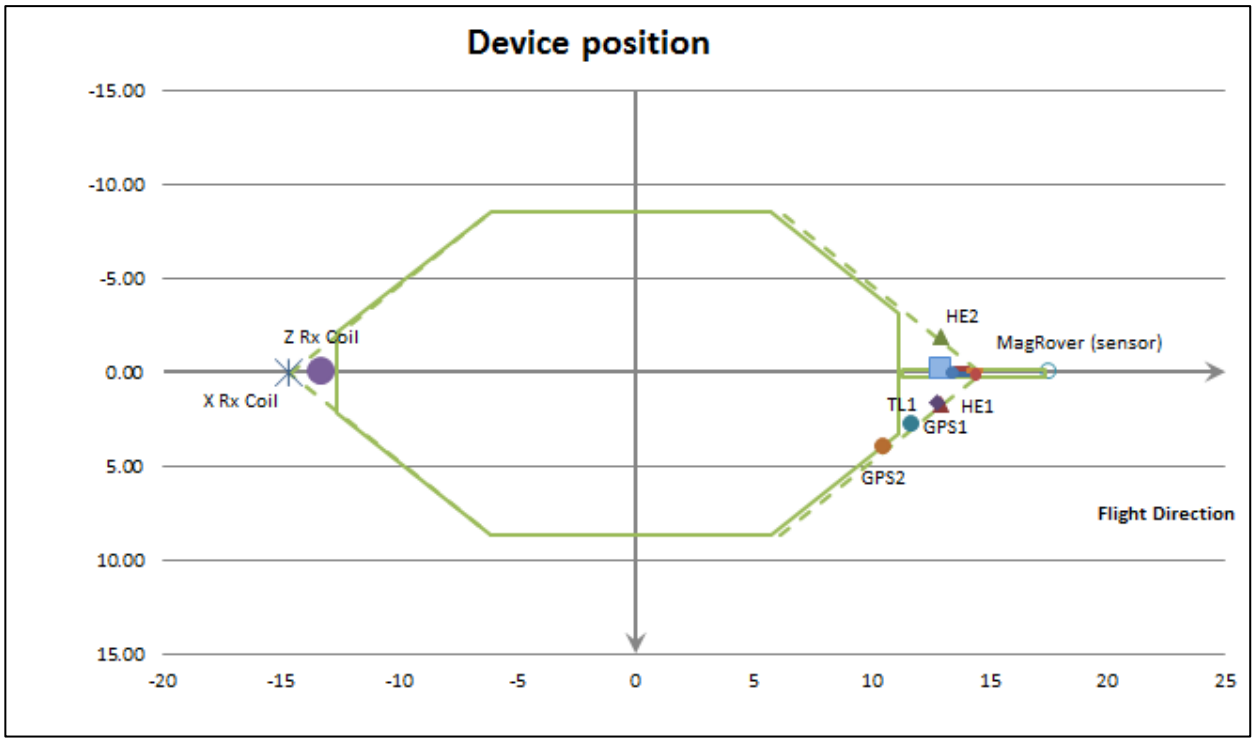

Figure 4 Sketch showing the frame and the position of the basic instruments. The green line defines the transmitter loop. The horizontal plane is defined by (x,y).

Ground base stations

The DGPS and magnetic base stations were positioned in the vicinity of the survey area at Coolidge airport.

DGPS base station

DGPS base stations were placed at a location of maximum possible view to satellites and away from metallic objects that could influence the GPS antenna.

Table below shows the location of the DGPS base station:

Area	Easting (m)	Northing (m)	Ellipsoidal height (m)
Que Block	595573.3	6708960.8	800.4 m

Magnetometer base station

The base station magnetometer was placed in a location of low magnetic gradient, away from electrical transmission lines and moving metallic objects, such as motor vehicles and aircrafts.

The table below shows the location of the magnetic base station:

Magnetometer Base station	Easting (m)	Northing (m)	Elevation (m)
Que Block	595574.53	6708954.61	802 m

Data Acquisition

The SkyTEM 312M system setup is a dual moment configuration containing a Low Monent (LM) with a peak moment of ~3.000 NIA and a High Moment (HM) with a peak moment of ~500.000 NIA.

A dual moment system provides a major advantage over single moment systems in that it is possible to measure a wider range of time gates. In LM mode early time gates can be measured allowing more accurately resolution in the near surface while in the HM mode, deep penetration can be achieved.

Data from two GPS receivers are recorded by the EM data acquisition system while a third GPS is recorded by the magnetic data acquisition system.
The DGPS system is used for time stamping, positioning, and correlation of the EM and magnetic datasets. All recorded data are marked with a time stamp used to link the different data types.

The time stamp is in UTC/GMT and the formats are either,

- Date and Time defined as; yyyy/mm/dd hh:mm:ss.sss
  or
- Datetime values defined as the number of days since 1900-01-01 and seconds of the day; ddddd.sssssssss

Gate times

Raw and calibrated gate times for low moment and high moment are presented in Table 8 and Table 9, respectively. All times are referred to start of turnoff of ramp down.

The earliest gates are not used as these are in the transition zone during the down ramp of the pulse.

If third party processing or inversions are undertaken using the processed data (Geosoft GDB) as the base dataset, the calibrated gate center times found in Table 8 and Table 9 for LM and HM, respectively, must be applied. Calibration is described in the following section.

Aarhus Workbench applies gate times and calibrations automatically as defined in the geometry file (.gex).

Gate #	Gate width (µs)	Raw Gate center (µs)	Calibrated LM Gate center (µs)	Comment
1	0.57	0.715	-1.375	Not Used
2	1.57	2.215	0.125	Not Used
3	1.57	4.215	2.125	Not Used
4	1.57	6.215	4.125	Not Used
5	1.57	8.215	6.125	Not Used
6	1.57	10.215	8.125	Not Used
7	1.57	12.215	10.125	Not Used
8	2.57	14.715	12.625	Not Used
9	3.57	18.215	16.125	LM
10	4.57	22.715	20.625	LM
11	5.57	28.215	26.125	LM
12	7.57	35.215	33.125	LM
13	9.57	44.215	42.125	LM
14	12.57	55.715	53.625	LM
15	15.6	70.2	68.110	LM
16	19.6	88.2	86.110	LM
17	24.6	110.7	108.610	LM
18	30.6	138.7	136.610	LM
19	39.6	174.2	172.110	LM
20	50.6	219.7	217.610	LM
21	62.6	276.7	274.610	LM
22	80.6	348.7	346.610	LM
23	100.6	439.7	437.610	LM
24	126.6	553.7	551.610	LM
25	160.6	697.7	695.610	LM
26	201.6	879.2	877.110	LM
27	254.6	1107.7	1105.610	LM
28	321.6	1396.2	1394.110	LM

Table 8 Gate times, Low Moment.

Gate #	Gate width (µs)	Raw Gate center (µs)	Calibrated HM Gate center (µs)	Comment
1	0.57	350.715	349.215	Not Used
2	1.57	352.215	350.715	Not Used
3	1.57	354.215	352.715	Not Used
4	1.57	356.215	354.715	Not Used
5	1.57	358.215	356.715	Not Used
6	1.57	360.215	358.715	Not Used
7	1.57	362.215	360.715	Not Used
8	2.57	364.715	363.215	Not Used
9	3.57	368.215	366.715	Not Used
10	4.57	372.715	371.215	Not Used
11	5.57	378.215	376.715	Not Used
12	7.57	385.215	383.715	Not Used
13	9.57	394.215	392.715	Not Used
14	12.57	405.715	404.215	Not Used
15	15.57	420.200	418.715	Not Used
16	19.57	438.200	436.715	Not Used
17	24.57	460.700	459.215	HM
18	30.57	488.700	487.215	HM
19	39.57	524.200	522.715	HM
20	50.57	569.700	568.215	HM
21	62.57	626.700	625.215	HM
22	80.57	698.700	697.215	HM
23	100.57	789.700	788.215	HM
24	126.57	903.700	902.215	HM
25	160.57	1047.700	1046.215	HM
26	201.57	1229.200	1227.715	HM
27	254.57	1457.700	1456.215	HM
28	321.57	1746.200	1744.715	HM
29	405.57	2110.200	2108.715	HM
30	510.57	2567.100	2567.215	HM
31	645.57	3147.200	3145.715	HM
32	791.57	3866.200	3864.715	HM
33	967.57	4746.200	4744.715	HM
34	1184.57	5777.100	5821.215	HM
35	1451.57	7141.200	7139.715	HM
36	1775.57	8755.200	8753.715	HM
37	2179.57	10733.200	10731.715	HM

Table 9 Gate times, High Moment.

System Verification

To verify the performance of the SkyTEM 312M system calibration and waveform repetition is carried out. The following sections document the results.

Calibration

The SkyTEM 312M system has been calibrated at the Danish National Reference site. Calibration includes measurements of the transmitter survey data repeated at a range of altitudes at the reference site. Hereby, it is documented that the instrumentation can reproduce the reference site with the same set of calibration parameters independent of the flight altitude. All processed data are corrected according to the calibration parameters.

The calibration resulted in the following parameters:

Low Monent
Multiplicative shift factor: 0.94 (on the raw dB/dt data)
Additive time shift: -1.99e-6 s (on gate times)

LM Calibrated gates center = Raw gates center -1.99e-6 s

High Moment
Multiplicative shift factor: 0.94 (on the raw dB/dt data)
Additive time shift: -1.8e-6 s (on gate times)
Down ramp time: 350 µs

HM Calibrated Gates Center = Raw HM gates -1.8e-6 s

The reference data for both LM and HM data are shown as grey curves and the measured data for LM and HM as green and blue curves, respectively, on Figure 5 to Figure 10.

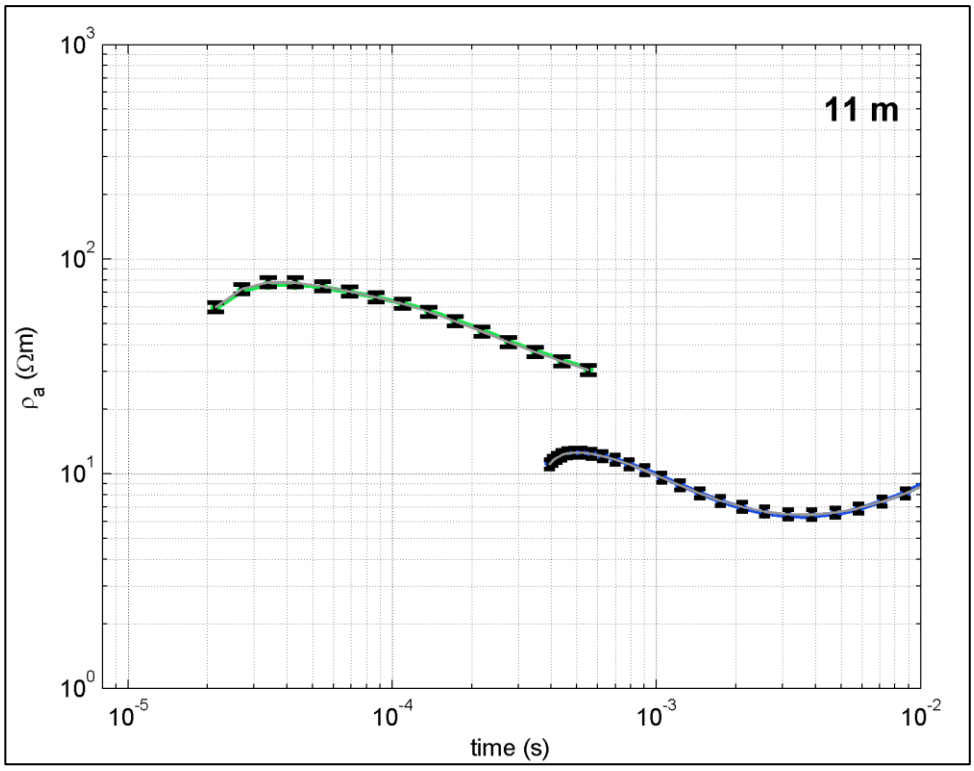

Figure 5 Grey curves with 5% error bars are the expected response, and green curves (LM) and blue curves (HM) are the actual measurements.

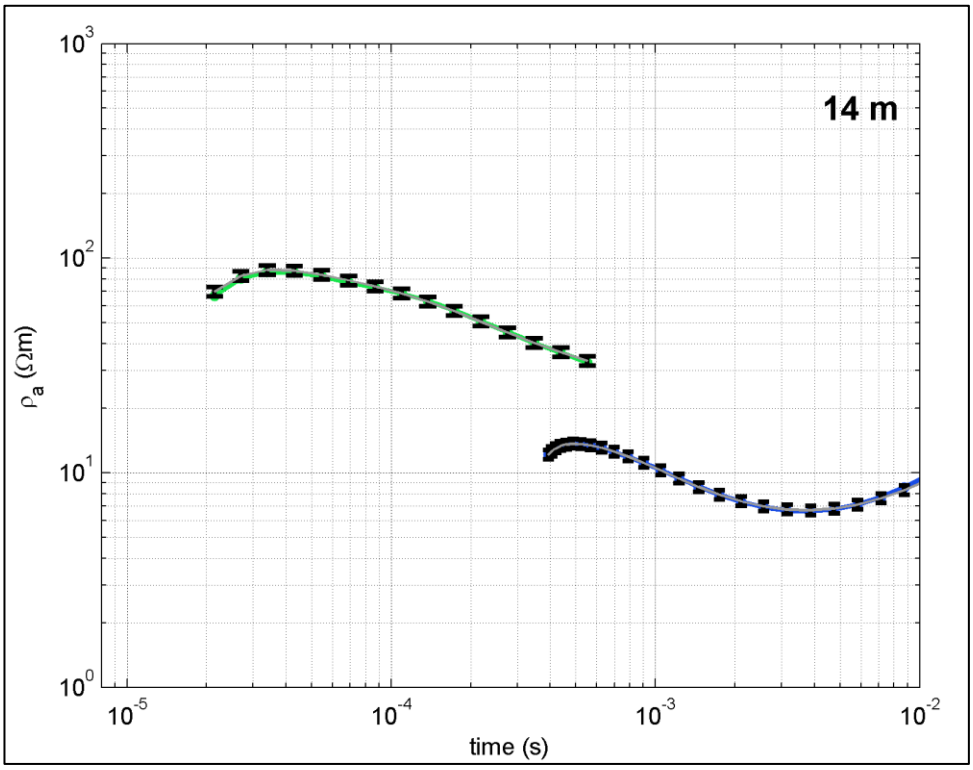

Figure 6 Grey curves with 5% error bars are the expected response, and green curves (LM) and blue curves (HM) are the actual measurements.

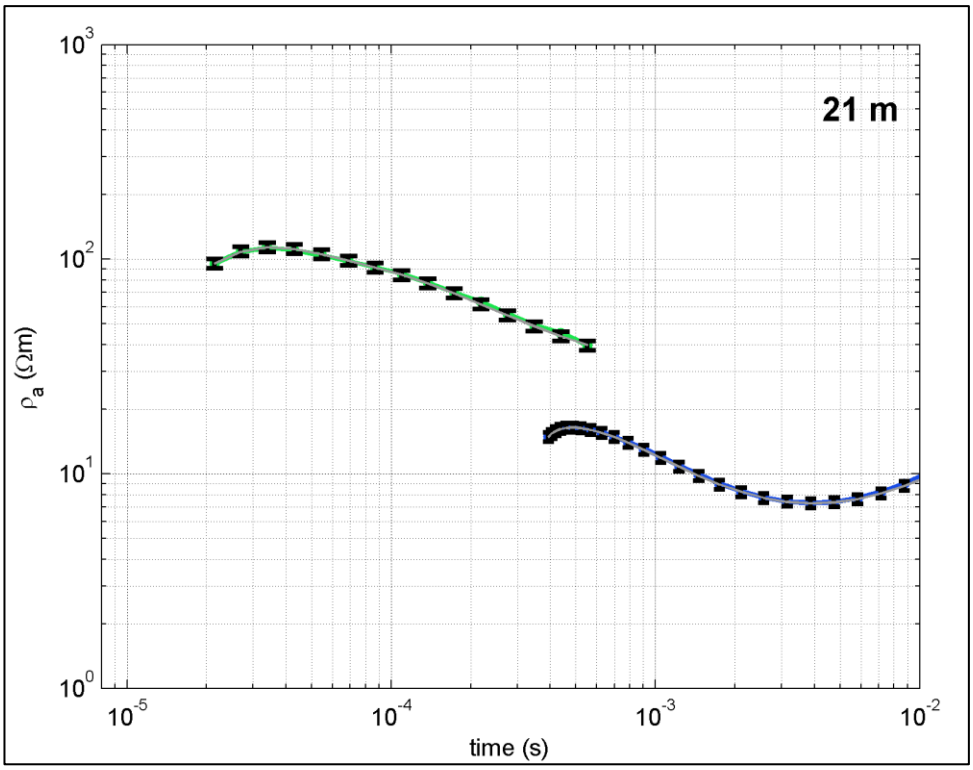

Figure 7 Grey curves with 5% error bars are the expected response, and green curves (LM) and blue curves (HM) are the actual measurements.

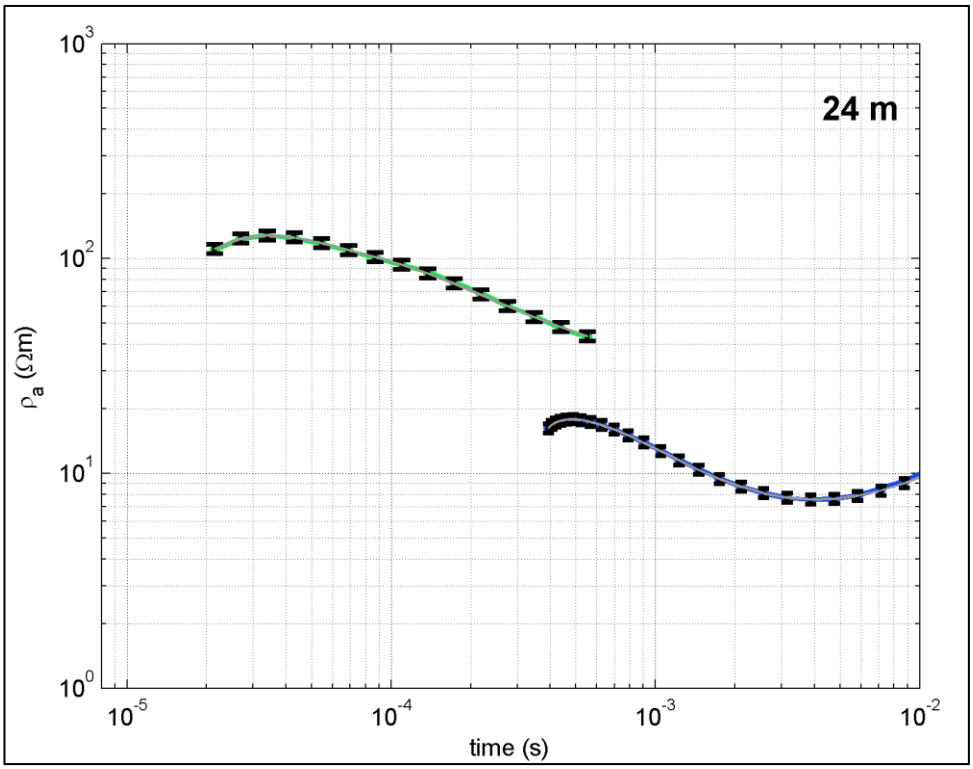

Figure 8 Grey curves with 5% error bars are the expected response, and green curves (LM) and blue curves (HM) are the actual measurements.

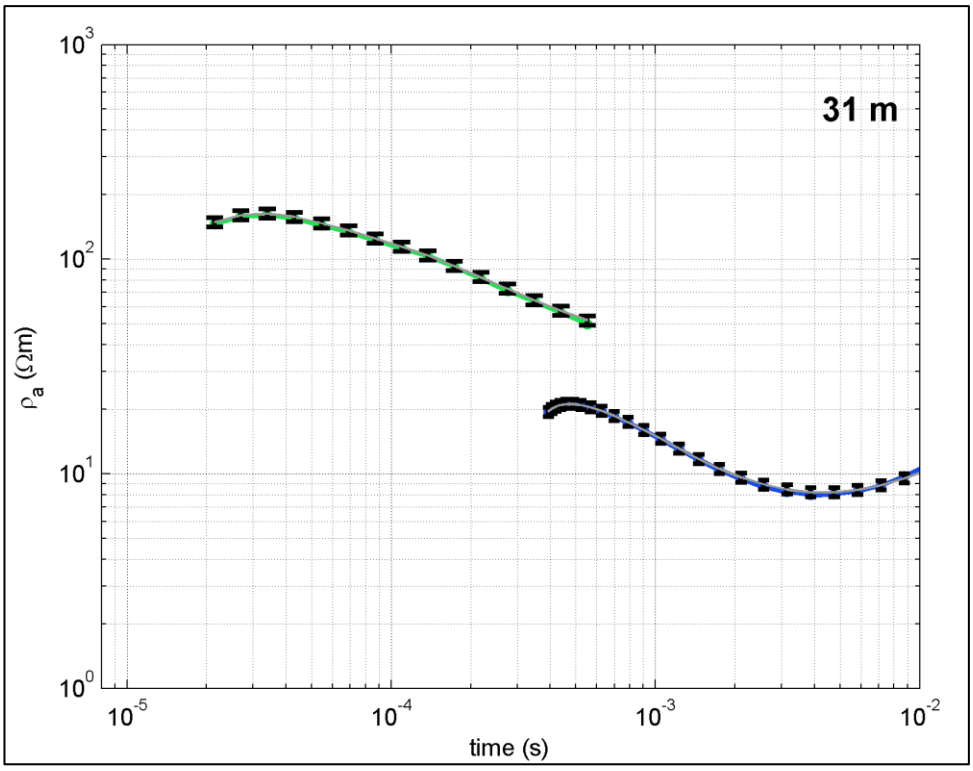

Figure 9 Grey curves with 5% error bars are the expected response, and green curves (LM) and blue curves (HM) are the actual measurements.

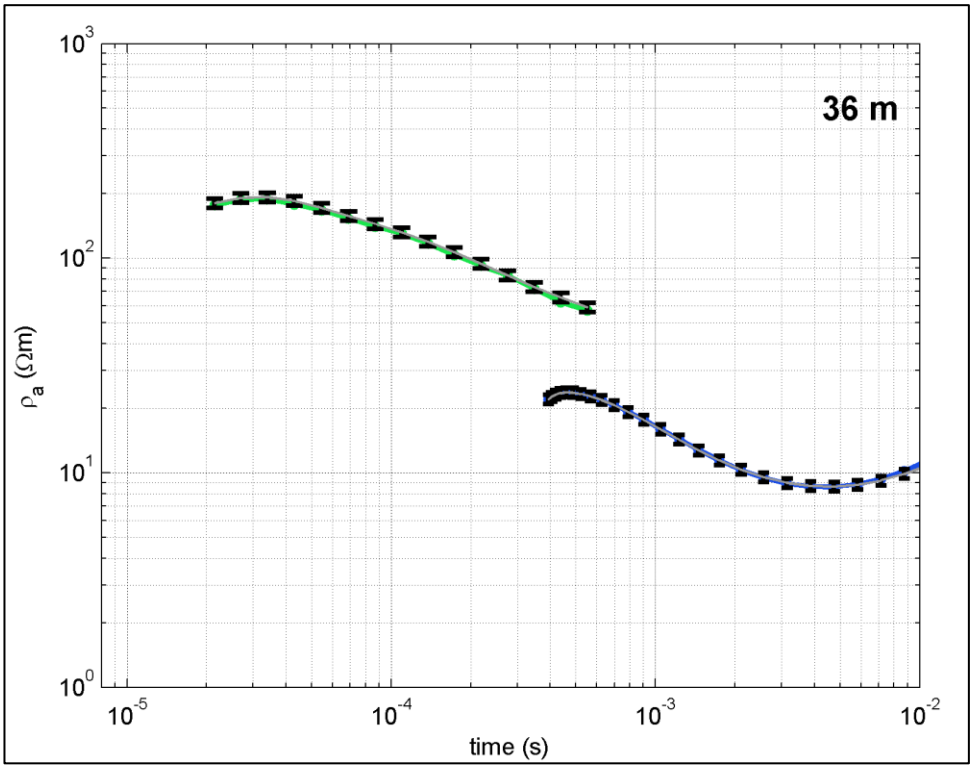

Figure 10 Grey curves with 5% error bars are the expected response, and green curves (LM) and blue curves (HM) are the actual measurements.

Waveform

The waveforms applied in the forward modelling are presented below.

The LM waveform is modelled based on the PFC analysis. Approximations to those waveforms are applied in modelling of the EM data. Figure 11 and Figure 12 show the approximated up and down ramps. Waveform details are presented in Table 10 to Table 13.

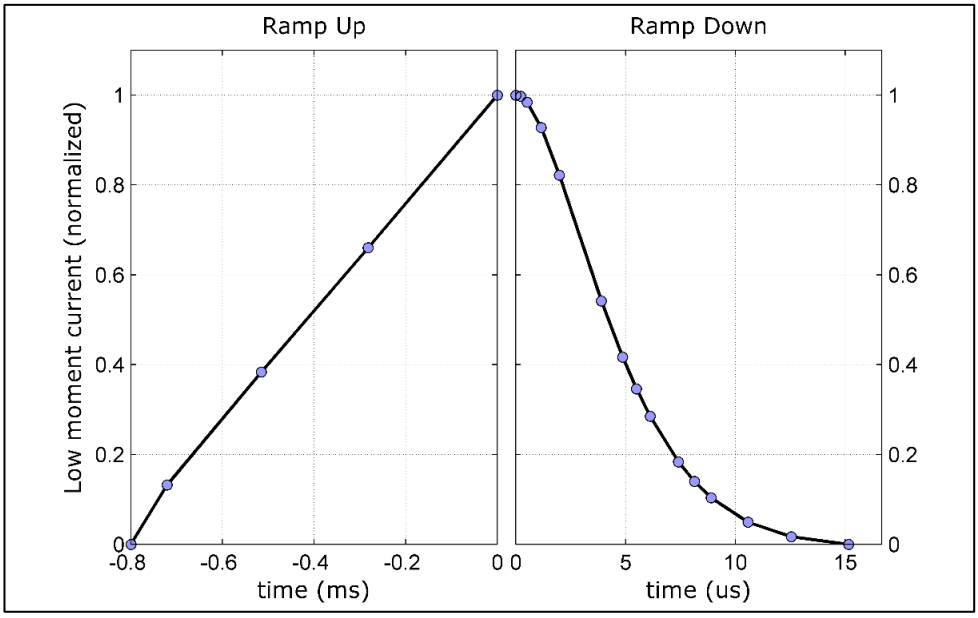

Figure 11 Ramp up and down at 210 Hz (LM). The current is normalised.

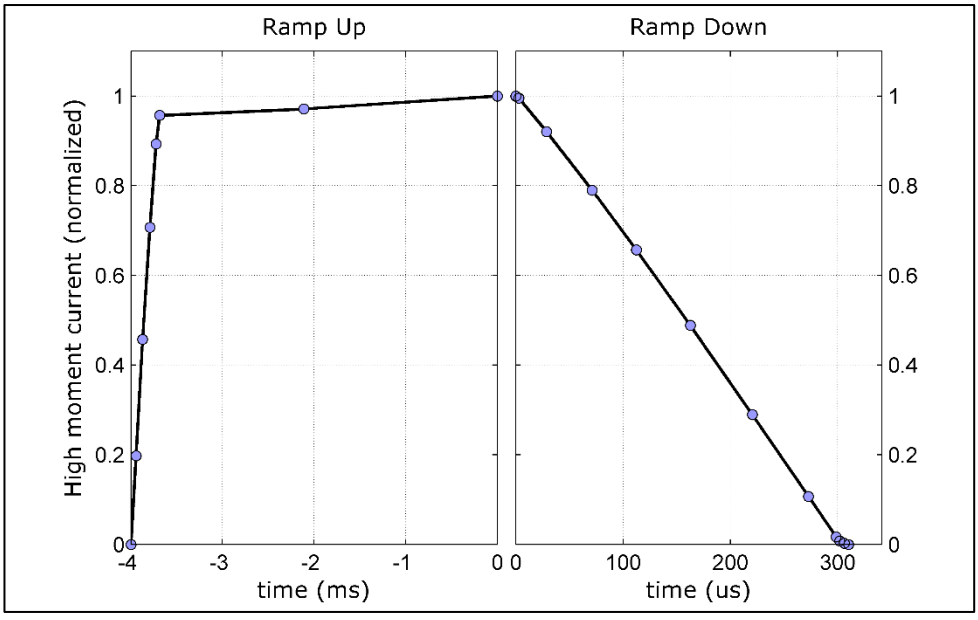

Figure 12 Ramp up and down at 30 Hz (HM). The current is normalised.

LM

Parameter	Value
Base frequency	210 Hz
Current range	6 amp

Table 10: Waveform parameters for LM

Time [s]	Normalized current
-8.00000E-04	0.00000E+00
-7.64730E-04	6.34310E-02
-6.28180E-04	2.49710E-01
-4.34970E-04	4.74530E-01
-9.21970E-05	8.90440E-01
0.00000E+00	1.00000E+00
2.10000E-07	9.96871E-01
4.80000E-07	9.79684E-01
1.07000E-06	9.10782E-01
1.66000E-06	8.16843E-01
3.26000E-06	5.36849E-01
3.84000E-06	4.47448E-01
4.41000E-06	3.69370E-01
5.43000E-06	2.54898E-01
6.50000E-06	1.66864E-01
7.19000E-06	1.24730E-01
7.92000E-06	9.02857E-02
9.59000E-06	4.04000E-02
1.16200E-05	1.28292E-02
1.45600E-05	0.00000E+00

Table 11: Normalized current for LM

HM

Parameter	Value
Base frequency	30 Hz
Current range	110 Amp

Table 12: Waveform parameters for HM

Time [s]	Normalized current
-4.00000E-03	0.000000
-3.94753E-03	0.192432
-3.89507E-03	0.371882
-3.84260E-03	0.538551
-3.79013E-03	0.692361
-3.73767E-03	0.833236
-3.68520E-03	0.961100
0.00000E+00	1.000000
5.28000E-05	0.844810
1.05600E-04	0.683233
1.58400E-04	0.516627
2.11200E-04	0.346352
2.64000E-04	0.173764
3.14900E-04	0.006606
3.16692E-04	0.003029
3.18759E-04	0.000000

Table 13: Normalized current for HM

Digital Data

The complete dataset of the SkyTEM survey is delivered as a Geosoft database (GDB) which can be used as input for further processing and gridding and as input to inversion and interpretation software. The channels of the GDB are described in Table 14.

Channel description**, Survey Data**

Parameter	Explanation	Unit
Fid	Unique Fiducial number	seconds
Line	Line number	LLLLLL
Flight	Name of flight	yyyymmdd.ff
DateTime	DateTime format	Decimal days
Date	Date	yyyymmdd
Time	Time	hhmmss.zzz
AngleX	Angle in flight direction	Degrees
AngleY	Angle perpendicular to flight direction	Degrees
Height	Filtered height measurement	Meters
Lon	Latitude/Longitude, WGS84	Decimal degrees
Lat	Latitude/Longitude, WGS84	Decimal degrees
E*	UTM Zone 8N (WGS84)	Metre
N*	UTM Zone 8N (WGS84)	Metre
DEM	Digital Elevation Model	M. a. sl.
Alt	DGPS Altitude	M. a. sl.
GdSpeed	Ground Speed	[km/h]
Curr_LM	Current, low moment	Amps
Curr_HM	Current, high moment	Amps
LM_Z [xx]**	Geosoft array channels. Normalized LM Z-coil value.	pV/(m4*A)
HM_Z [xx]**	Geosoft array channels Normalized HM Z-coil value.	pV/(m4*A)
HM_X [xx]**	Geosoft array channels Normalized HM X-coil value.	pV/(m4*A)
LM_X [xx]**	Geosoft array channels Normalized LM X-coil value.	pV/(m4*A)
Tau	Adaptive Tau Calculation, on HMZ	msec
LastGate	Last gate used in the Tau calculation	Gate number
_60Hz_Intensity	Amplitude spectral density of the power line noise 60 Hz	-
Mag_Raw	Total Magnetic Intensity Raw magnetic data	nT
TMI	Final Total Magnetic Intensity	nT

RMI	Residual magnetic Field IGRF corrected based on 2015 model Final corrected data	RMI
Diurnal IGRF	Diurnal variation Magnetic base station data IGRF value 2015 mode;	nT nT
Inc	IGRF Inclination	degrees
Dec	IGRF Declination	degrees

Table 14 Channel description, survey data

**) Data positions refer to the center of the frame.*

***) The first valid gates are: 9 (LM), 17 (HM).*

Inversion results

The result of the Surface constrained inversion is delivered as a Geosoft database (GDB) containing the modelled layer conductivity's. The channels of the GDB and XYZ-files are described in Table 15.

The applied gridding methods, cell size, blanking distance and filtering are listed in Table 16.

Channel description, EM inversion database

Parameter	Explanation	Unit
Line	Line number	LLLLLL
E	UTM Zone 8N (WGS84)	Metre
N	UTM Zone 8N (WGS84)	Metre
DTM	Digital Terrain Model	Meters above mean sea level
ResI1	Residual of data	-
Height	Filtered Height Measurement	Metre
InvHei	Inverted Height	Metre
DOI	Depth of Investigation below surface	Metre
DOI_Elevation	Depth of Investigation below elevation	Metre
Elev_[xx]	Elevation of top of layer xx	Metre
Con_[xx]	conductivity of layer xx	mS/m
Con_[xx]_doi	Masked below DOI of layer xx	mS/m
Elev_array	Elevation of each depth	Metre
RUnc_[xx]	Relative uncertainty of layer xx	-

Table 15 Channel description, inversion results

Gridding method and parameters

Area	Gridding algorithm	Gridding filter	Cell size	Blanking distance
Que Block	Minimum curvature	-NA	20 m	600 m

Table 16: Geosoft gridding

Data processing and presentation

This section covers processing of auxiliary data and processing and inversion of EM data and presentations.

All devices (DGPS, Laser altimeters, inclinometers) are moved to the centre of the frame and corrected for the tilt of the frame hence all data positions refer to the center of the frame. Data is split at the beginning and end of each planned flight line.

After the initial filtering all data are resampled to 10Hz.

Auxiliary data

Tilt processing

The X and Y angle processing involves manual and automated routines using a combination of the SkyTEM in-house software SkyLab and Geosoft.
The processing involves the following steps:

1. 3 sec box filter (SkyLab)
2. Low pass filtering of 3.0 sec. (Geosoft)

Height processing

The height processing involves manual and automated routines using a combination of the SkyTEM in-house software SkyLab and Geosoft.
The processing involves the following steps:

1. Keeping the 5 highest values pr. second and discarding the rest to correct for the canopy effect (treetop filter) (SkyLab)
2. 3 sec running box filter (SkyLab)
3. Tilt correction (SkyLab)
4. Averaging of the two laser values (SkyLab)
5. Additional filters:
    a. Low pass filter of 3.0 sec (Geosoft)

DGPS processing

The DGPS has been processed using the Waypoint GrafNav Lite Differential GPS processing tool. The standard airborne settings have been used.

1. Import of base station (Master)
2. Import of airborne files (Rover)
3. Calculation of forward and reverse DGPS solution
4. Export as .txt file

The DGPS.txt files are used as input to the SkyLab software assuring DGPS corrected data in the processed files.

The ground speed, altitude, latitude and longitude from the processed DGPS' are imported into Geosoft and merged into the final database, where the coordinates are converted into UTM Zone 8N (WGS84) and a low pass filter of 3.0 sec is applied.

Digital elevation model

A digital elevation model (DEM) has been calculated by subtracting the filtered laser altimeter data from the DGPS elevation. All steps related to the DEM are carried out Geosoft.

The processing of the final DEM involves the following steps:

1. Filtering and processing of the laser altimeter height as described above
2. DEM data received by subtraction of final filtered laser data from final processed DGPS altitude data

Figure 13 shows the DEM for the survey area.

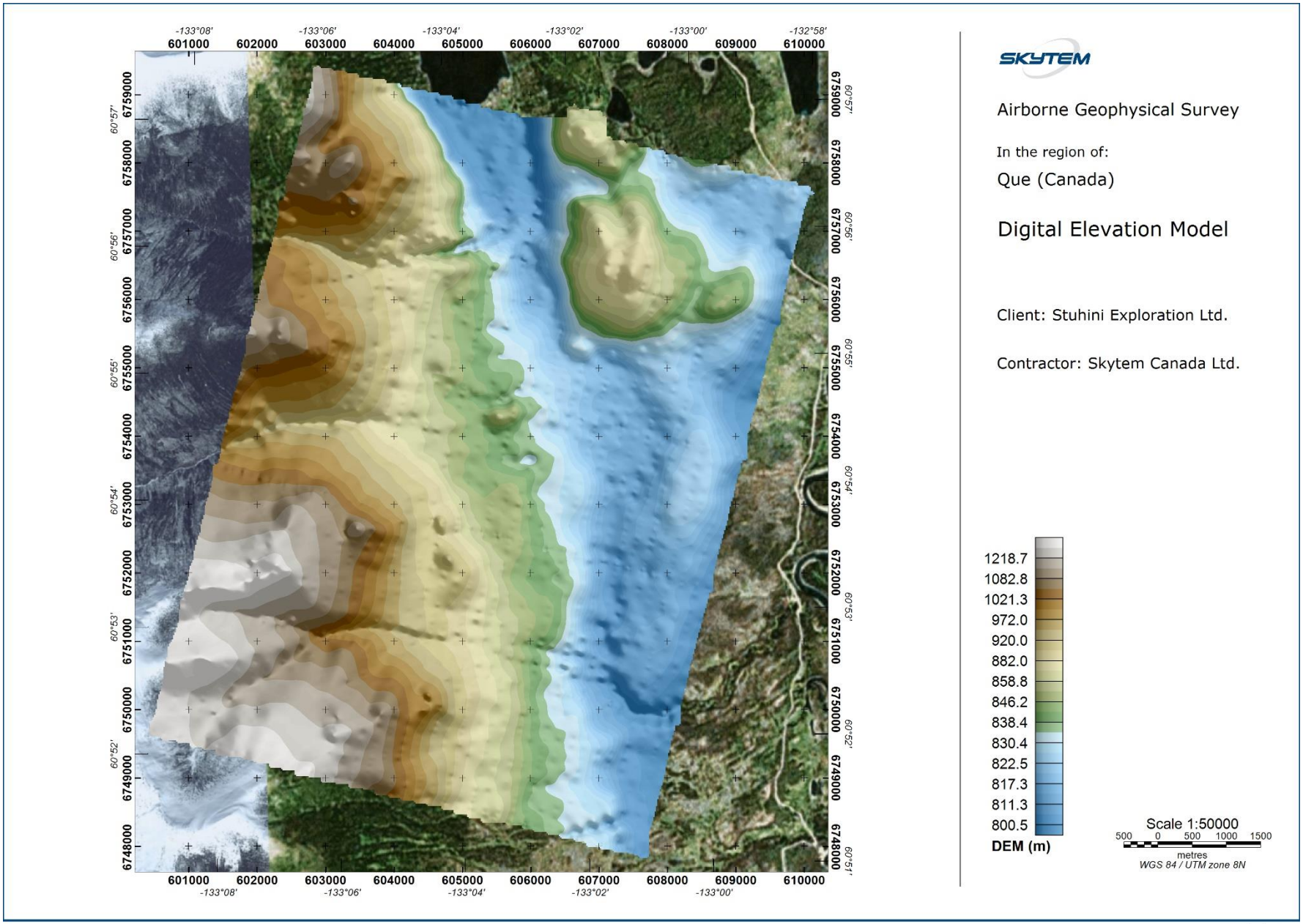

Figure 13 Digital Elevation Model (DEM) in meter above sea level.

Magnetic data

Final processing of the magnetic data involves the application of traditional corrections to compensate for diurnal variation and heading effects prior to gridding.
Geosoft magnetic data processing tools are applied as follows:

- Processing of static magnetic data acquired on magnetic base station
- Pre-processing of airborne magnetic data
    - Stacking of data to 10 Hz in SkyLab.
    - Moving positions to the center of the system in SkyLab.
- Processing and filtering of airborne magnetic data
- Standard corrections to compensate the diurnal variation
- IGRF correction
- Gridding
- No heading correction applied.

Processing of base station magnetic data

The base station magnetometer data was merged into the base station Geosoft database on a daily basis for further processing.

The following filtering was applied:

- Manual despiking to remove spikes
- Interpolation (Geosoft Akima)
- Fraser Low-pass filter (width 60 sec)
- Diurnal variations are calculated by subtracting 56346.1 nT.

Processed residual magnetic data from the magnetic base station representing short term variations was merged together with airborne magnetic data.

Processing and Filtering of airborne magnetic data

Airborne magnetic data is filtered and interpolated as follows:

- Adjustment of the data for the time lag between the GPS position and the position of the magnetic sensor.
- Data resampling to 10 Hz (stacking)
- Manual despiking to remove spikes and spurious data
- Geosoft processing:
    - Akima interpolation
    - Fraser Low-pass filter (width 3 sec)

Corrections to the magnetic data

The following corrections are applied to the airborne magnetic data:

- Correction for diurnal variation using the digitally recorded ground base station magnetic values as described above
- Lag was negligible and no lag correction was applied
- Heading was negligible and no heading correction was applied
- IGRF correction
- Micro-levelling was not applied

The result is the Residual Magnetic Field data (RMF)

IGRF correction

The International Geomagnetic Reference Field (IGRF) is a long-wavelength regional magnetic field calculated from permanent observatory data collected around the world. The IGRF is updated and determined by an international committee of geophysicists every 5 years. Secular variations in the Earth's magnetic field are incorporated into the determination of the IGRF.

The IGRF model is calculated before levelling using the following parameters:

IGRF model year: 2015, IGRF 15th generation
Date: variable according to date channel in database
Position: variable according to GPS WGS84 longitude and latitude
Elevation: variable according to magnetic sensor altitude derived from DGPS data

TMI

Total magnetic intensity (TMI) data was created by diurnally correcting the airborne magnetic data.

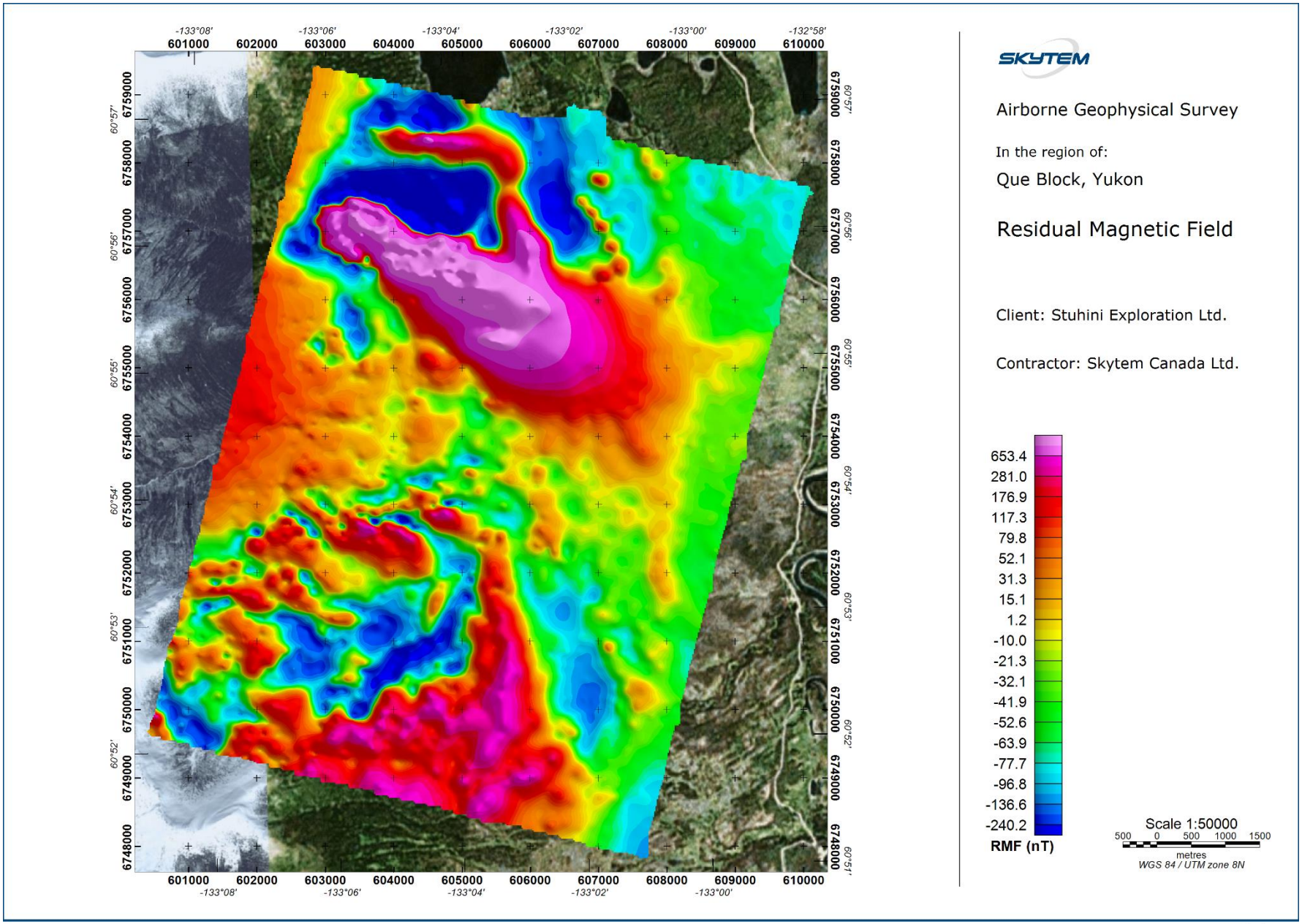

Figure 14 Residual Magnetic Field

Power Line Noise Intensity (PLNI)

The PLNI is a powerful tool for identifying power line noise effect on EM and magnetic data. The PLNI monitor values are derived from a frequency analysis of the raw Z-component EM data. For every low moment EM data block a PLNI value is obtained by Fourier transformation of the measured values for the latest low moment gate. The Fourier transformation is evaluated at the local power transmission frequency yielding the amplitude spectral density of the power line noise.

CAUTION - When evaluating the PLNI values one should be aware of the following factors that may give rise to anomalous PLNI patterns unrelated to the actual power line noise level:

- The low moment EM data are measured at a rate lower than the Nyquist criterion for the applied system bandwidth which means that some of the frequency components contained may represent aliased frequencies. However, the considerable integration time of the latest low moment gate reduces this problem significantly.
- Other noise sources than power line noise may contribute to the total noise spectral density in the data at the power transmission frequency. When power line noise is present it tends to dominate all such other noise sources.
- The presented PLNI values are not corrected for fly height or frame angles, which means that adjacent lines crossing the same power line may not exhibit the same values of PLNI.

EM data

This section covers processing of EM data, including primary field correction (PFC) and filtering of EM data.

Primary Field Compensation (PFC)

The magnetic field coupling between the receiver coils and the transmitter loop is continuously hardware-monitored, providing a separate value for the magnetic field coupling during each transient sounding. These data are used for raw data correction in a separate post-processing step. The primary field compensation technique has proven stable and has routinely yielded a reduction of the primary field influence in very early time gates by a factor exceeding 50.

EM Filtering

The PFC data is the input for further processing. The data are normalized in respect to effective Rx coil area, Tx coil area, number of turns and current giving the unit [pV/(m^4*A)].

The EM data is filtered adaptively based on the signal-to-noise ratio. The applied EM filtering method is based on iterative weighted spline fitting routines, which operate in positive/negative symmetric transform spaces. The data weighting scheme relies on an extensive noise evaluation performed on the individual gate values of the raw data decays. Optimised sets of averaging filters are used for each measured moment and type of receiver coil in a stepwise averaging process. This allows for optimal suppression of motion induced noise as well as cultural noise components, while keeping track of the resulting data uncertainty.

Height correction

The provided EM grids are corrected for variations in flying height. The data has been adjusted as if it was flown at a constant 45m EM sensor height.

No height correction has been applied to the raw EM data channels in the delivered Geosoft database and data file.

Figure 15 shows an example of the LM Z data (Height corrected) of the block. Geosoft grids of EM Z channels are included in the digital data delivery.

Figure 16 shows an example of HM Z data (Height corrected). Geosoft grids of EM Z channels are included in the digital data delivery.

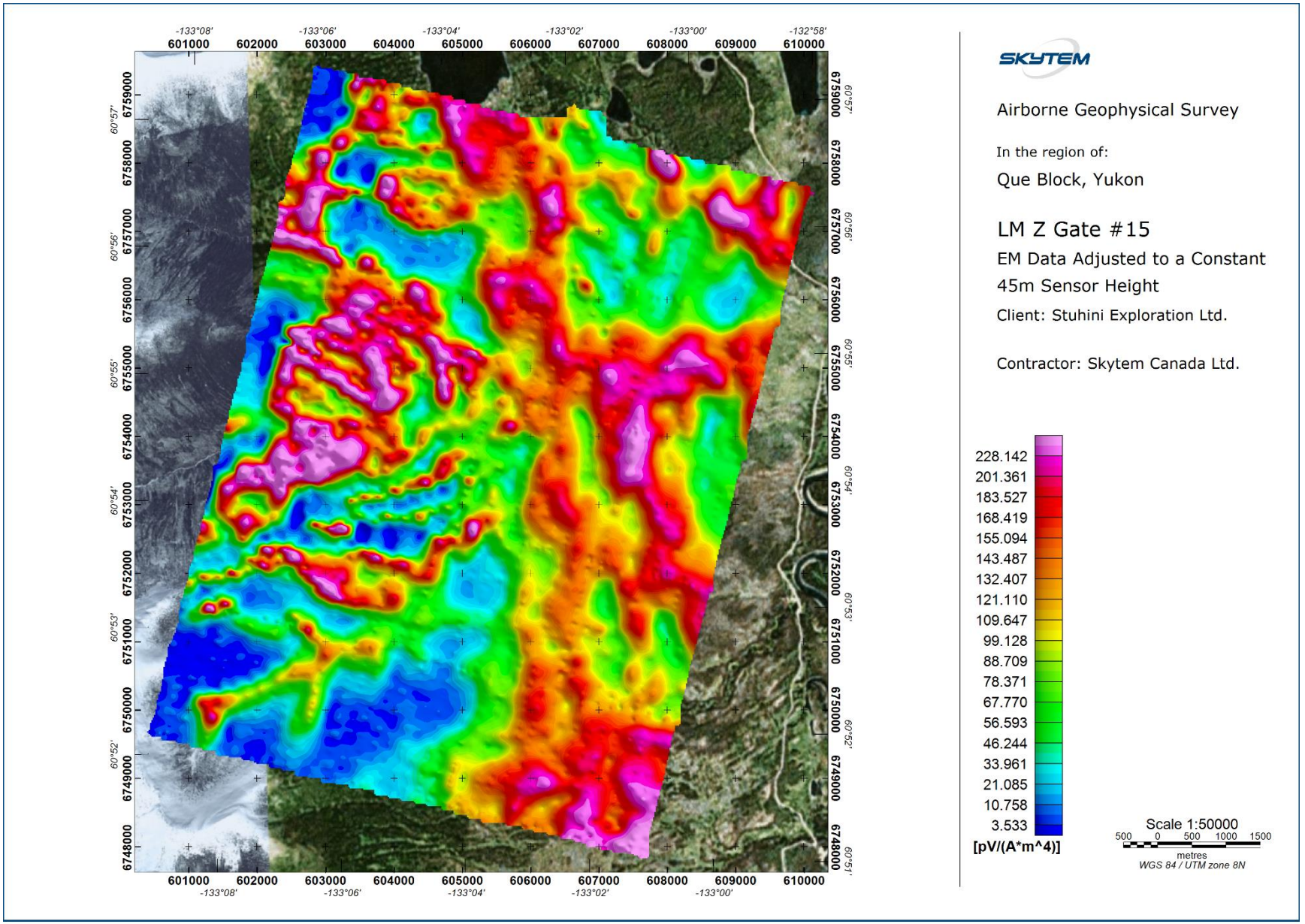

Figure 15.Low Moment Z coil (gate 15). Warm colours (red) represent high intensity.

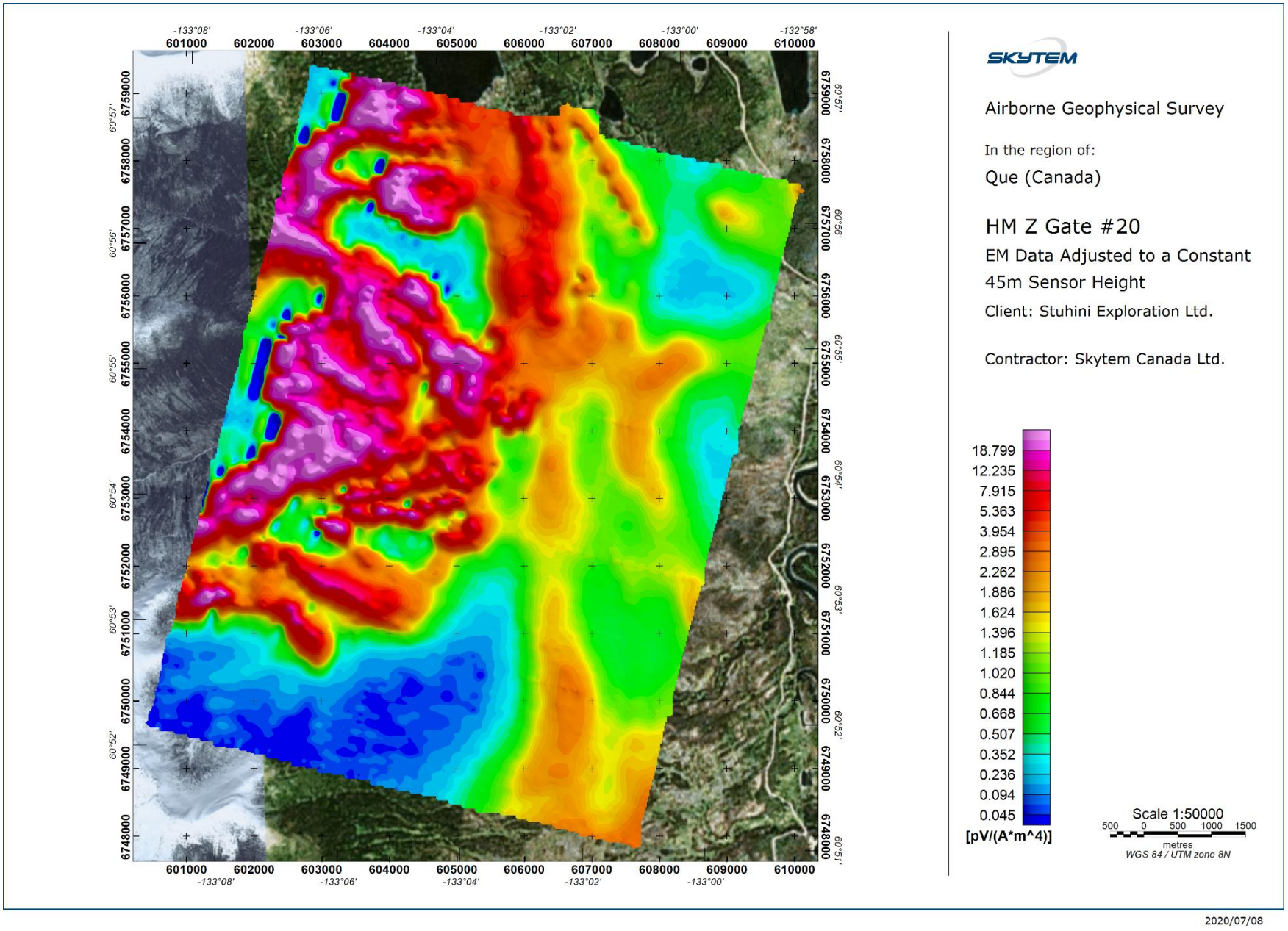

Figure 16. High Moment Z coil (gate 20). Warm colours (red) represent high intensity.

Time Constant

An adaptive Tau calculation has been performed on the HMZ data in the area and the result is presented in the map below as well as being included in the data delivery folder.

The adaptive Tau method treats each sounding curve individually and it involves the following steps for each sounding position:

- Identifying the latest gate with a relative data uncertainty below a user-defined threshold. Later gates are regarded as having too low S/N ratio to be reliably used in the subsequent fitting operation.
- Fitting an exponential function to a user-defined number of consecutive gates up to and including the latest gate defined above. The fitting procedure follows the latter formulation given in (1) using end-of-ramp referenced gate times.

For the present survey, the upper threshold for acceptable relative uncertainty is set to 0.35 and 4 consecutive gates are used in each exponential fit.

Inversion

In this section, the particulars of modelling and inversion of SkyTEM data from Que Block will be described with reference to the more general material found in Appendix 2.

The SkyTEM data have been processed and inverted using spatially constrained inversion (SCI) in Aarhus Workbench, a unique software package initially developed at Aarhus University, Denmark. In this SCI algorithm a group of time-domain EM (TEM) soundings are inverted simultaneously using 1-D models. Each sounding yields a separate layered model, but the models are constrained laterally.

The result of the SCI inversion is a model section that varies smoothly along and across the profiles and yields a conductivity model that combines the very good shallow depth resolution offered by the low moment data and the larger depth of investigation from the high moment data. See Figure 17.

---

(1) Weisstein, Eric W. "Least Squares Fitting--Exponential." From MathWorld--A Wolfram Web Resource. http://mathworld.wolfram.com/LeastSquaresFittingExponential.html

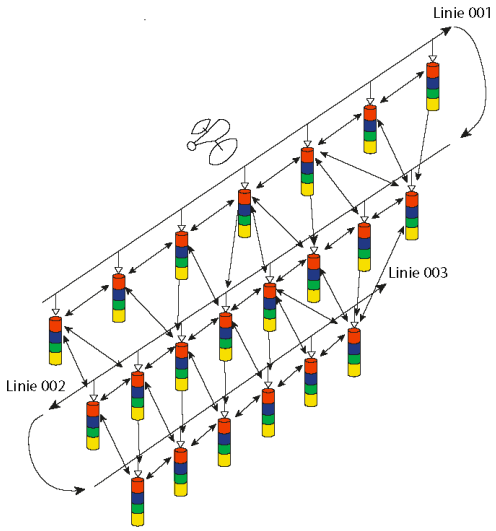

Figure 17. Schematic presentation of the SCI setup. Constraints connect not only soundings located along the flight line, but also those across them (figure from hgg.au.dk).

Initial model and optimisation norm

The SCI code is run in multi-layer, smooth-model mode in which the layer thicknesses are fixed and the data are inverted only for conductivity.

In the inversion the thickness of the first layer is set to 5 mand the depth to the top of the deepest layer boundary is 500 m. While computing the layer thicknesses, the first and last layer boundary scales the model thicknesses automatically using a log distribution. Thicknesses and depths to the top of each layer for the current project are given in the table below.

The input data to the inversion are the LM & HM moments of the Z-component of EM data. The initial model conductivity structure is a homogenous half-space model with an Auto Calculated starting conductivity.

Manually masking of data displaying coupling effects e.g. due to power lines is not part of the current project and therefore cultural effects in the EM data can be present in the final data base.

Layer #	Layer Thickness [m]	Depth to top of layer [m]
1	5	0
2	5.4	5
3	5.8	10.4
4	6.3	16.2
5	6.7	22.5

6	7.3	29.2
7	7.8	36.5
8	8.5	44.3
9	9.1	52.8
10	9.8	61.9
11	10.5	71.7
12	11.4	82.2
13	12.4	93.6
14	13	106
15	14	119
16	16	133
17	16	149
18	18	165
19	20	183
20	20	203
21	23	223
22	24	246
23	26	270
24	28	296
25	32	324
26	28	356
27	37	384
28	38	421
29	41	459
30	-	500

Table 17 Layer distribution of the multi-layer smooth inversion model.

Model Presentation - Model sections and maps

The models resulting from the inversion are presented as layer conductivity profiles and as grids and maps of mean conductivity in depth intervals in Geosoft and pdf format. Figure 18 and Figure 19 show examples of a layer conductivity profiles and maps respectively. All profiles, grids, images and maps are included in the digital data delivery.

Model Sections

The profile plots consist of four sections; the top section shows the inverted models, with topography, where the conductivity of the individual layers is colour coded according to the colour bar. The conductivity is shown on a logarithmic scale and conductive and resistive features appear with the same weight. The white shading in the analysis section indicates the estimated lower depth of investigation (DOI) and the gray curve the upper DOI. Where the colour fades into the white, the inverted

conductivity is determined almost exclusively by the regularization, i.e. the conductivity is essentially undetermined. The measured and inverted flight elevation is shown with a black and blue line, respectively, above the model section.

Below the model section are two plots of the measured data (dots) together with the response of the inverted models (solid lines). LM is low moment data and HM is high moment data.

The bottom section shows the data residual (black line) of the inversions.

Blank sections in the profile indicate areas where the signal to noise ratio has been too low for any data to be used in the inversion. Essentially the resistivity in those sections can be considered as "Very high" (>1000 Ωm). Alternatively, a man-made conductor has interfered with the signal which can also lead to data being discarded prior the inversion.

The quality of the inversion results can be evaluated by inspecting the residuals. The data residual is calculated by comparing the measured data with the response of the resulting model after inversion. If the residual is in the range of 1, the misfit between the response of the final model and the data is, on average, equal to the noise. If the residual is high, it might be caused by data that are noisier than the noise model takes into account. This can be seen where resistivity is very high and the signal consequently very low. A high data residual can also be due to the inconsistency between the 1D model assumed in the inversion and the 2D/3D character of the real world. These are found primarily at the edges of sharp lateral conductivity contrasts. Finally, coupling effects due to power lines and other manmade conductors can also be a source of a high residual.

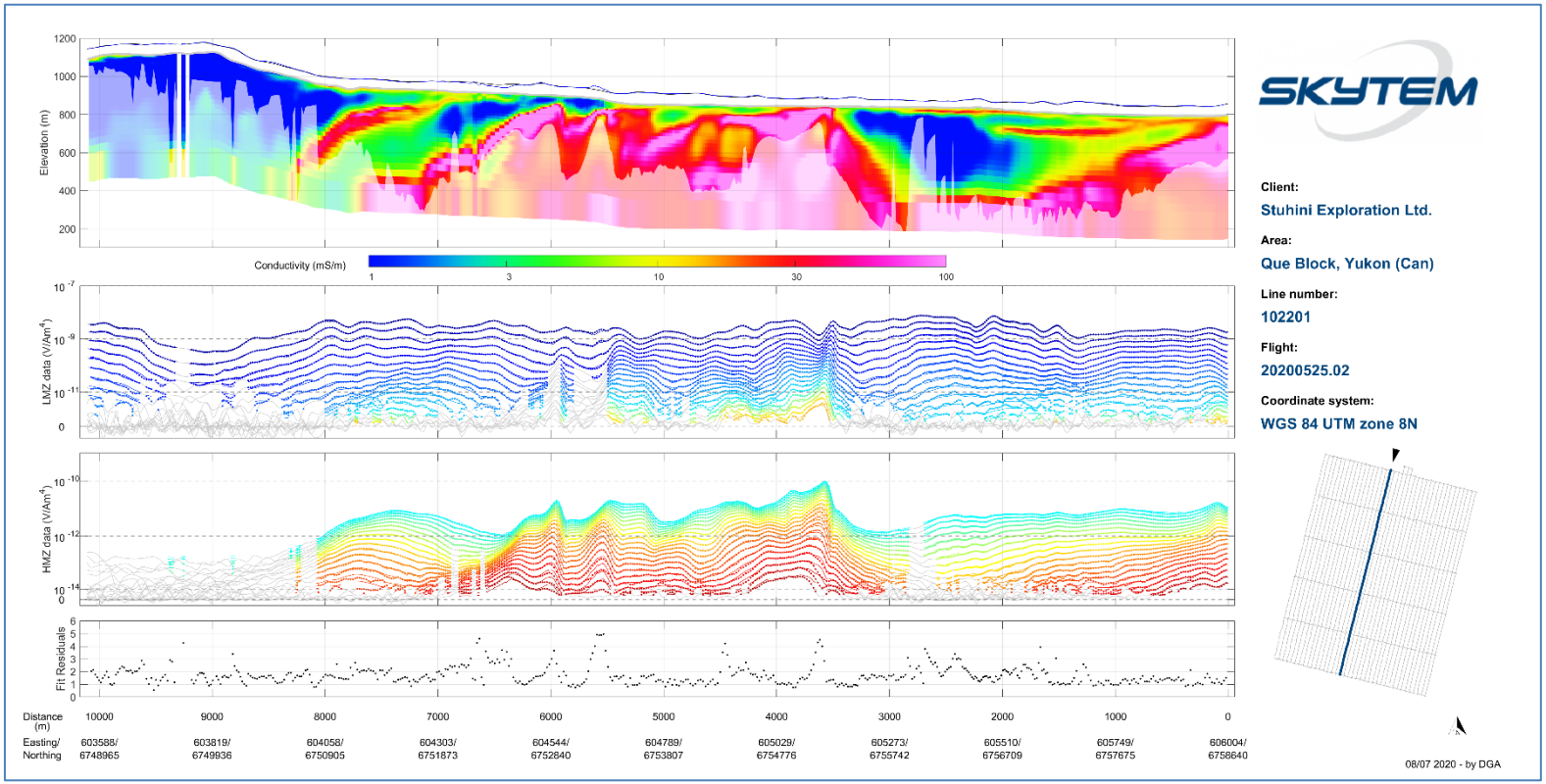

Figure 18 Example of section plot. From top to bottom: resistivity section with flight height and Depth of Investigation (DOI), LM gate plot (data=dots, model=line), HM gate plot (data=dots, model=line), residual.

Layer conductivity maps

The layer conductivity maps show the inverted resistivity for each of the model layers. As the thickness of the model layers increases downwards the maps represent a varying thickness interval. The depth intervals for each layer are stated on the maps in meters below the surface.

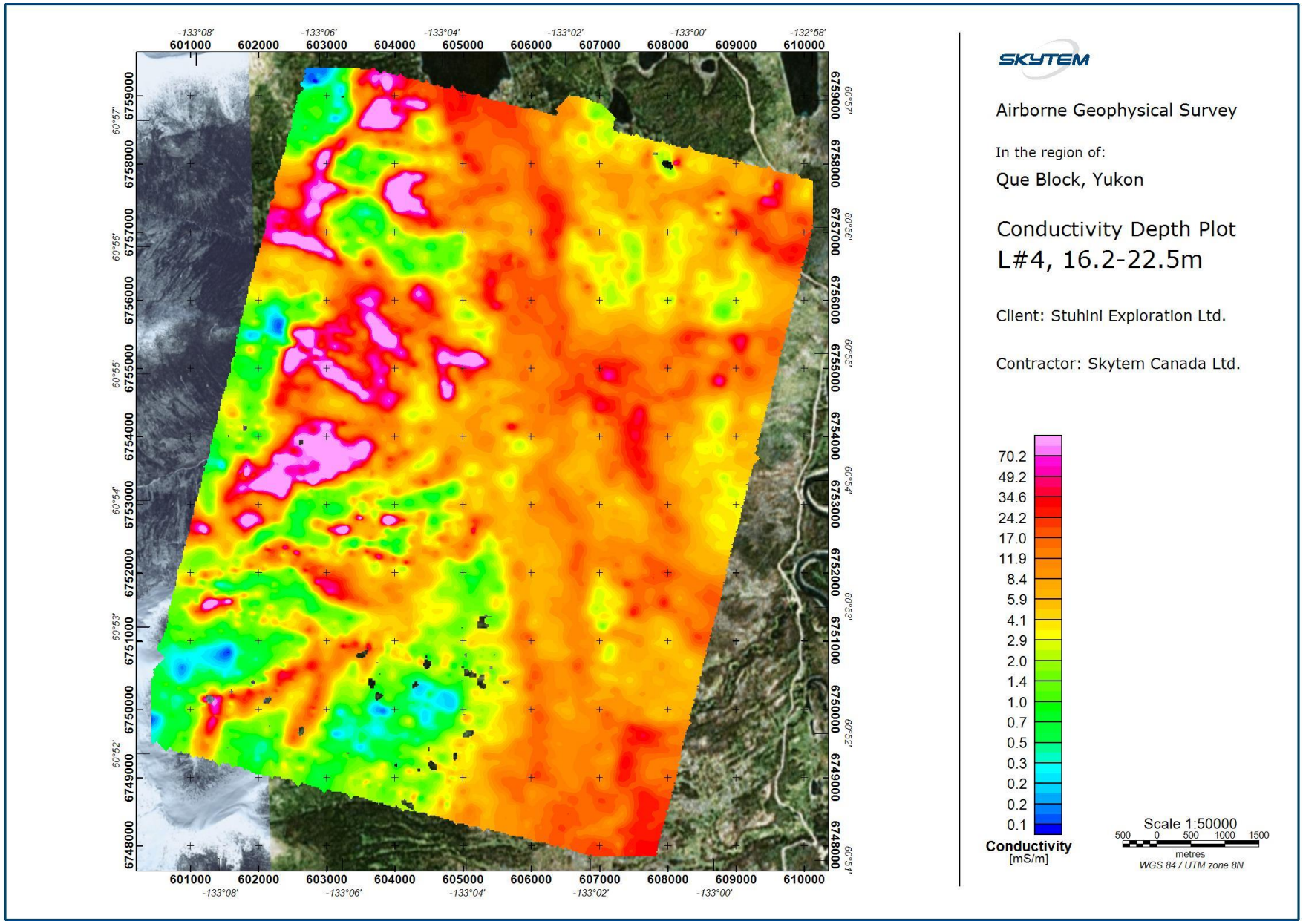

Figure 19. Modelled Layer Conductivity of layer 4.

References

Aarhus University, n.d., Guide to 1D-LCI inversion.

Auken, E., Foged, N. and Sørensen, K., 2002, Model recognition by 1-D laterally constrained inversion of resistivity data: Proceedings – New Technologies and Research Trends Session, 8th meeting, EEGS-ES.

Auken, E., Christiansen, A. V., Jacobsen, B. H., Foged, N., and Sørensen, K. I., 2005, Piecewise 1D Laterally Constrained Inversion of resistivity data: *Geophysical Prospecting*, 53, 497–506.

Christiansen, A.V. and Auken, E., 2012, A global measure for depth of investigation: *Geophysics,* vol 77, No. 4, 171-177.

Sattel, D., 2005, Inverting airborne electromagnetic (AEM) data with Zohdy's method, Geophysics, 70, G77-G85.

Viezzoli, A., Christiansen, A.V., Auken, E. and Sørensen, K., 2008, Quasi-3D modeling of airborne TEM data by spatially constrained inversion: *Geophysics,* vol 73, No. 3, F105-F113.

Appendix list

Appendix 1: Instruments

Appendix 2: Introduction to Spatially Constrained Inversion

Appendix 1: Instruments

Instrument positions

The instrumentation involves a time domain electromagnetic system, two inclinometers, two altimeters and two DGPS'.

The measurements were carried out, using a setup as described below.

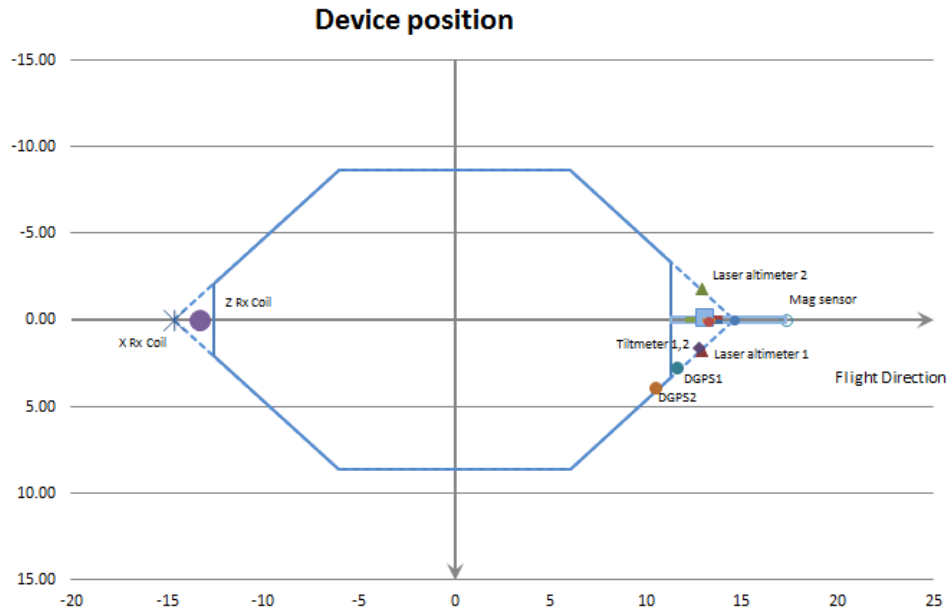

Figure 20 Sketch showing the frame and the position of the basic instruments. The blue line defines the transmitter loop. The horizontal plane is defined by (x, y).

The location of instruments in respect to the frame is shown in Figure 3 and is given in (x, y, z) coordinates in Table 1.

X and y define the horizontal plane. Z is perpendicular to (x, y). X is positive in the flight direction, y is positive to the right of the flight direction, and z is positive downwards.

The generator used to power the transmitter is suspended ~30 m below the helicopter and above the frame.

Device	X	Y	Z
DGPS1 (EM)	11.68	2.79	-0.16
DGPS2 (EM)	10.51	3.95	-0.16
HE1 (altim.)	12.94	1.79	-0.12
HE2 (altim.)	12.94	-1.79	-0.12
Inclinometer 1	12.79	1.64	-0.12
Inclinometer 2	12.79	1.64	-0.12
RX (Z Coil)	-13.25	0.00	-2.00
RX (X Coil)	-14.65	0.00	0.00
Mag sensor	20.50	0.00	-0.56

Table 18 Instrument locations.

Transmitter

The time domain transmitter loop can be described as an octagon with the corners listed in Table 19.

X	Y
-12.64	-2.10
-6.14	-8.58
6.14	-8.58
11.41	-3.31
11.41	3.31
6.14	8.58
-6.14	8.58
-12.64	2.10

Table 19 Corners of the transmitting loop.

The total area of the transmitter coil defined by the corner points is 342 m² and 68.3 m in circumference.

The key parameters defining the transmitter are listed in Table 20 and Table 21.

Low Monent

Parameter	Value
Number of transmitter turns	2
Transmitter area	342 m²
Peak current	6 amp
Peak moment	~3.000 NIA
Repetition frequency	210 Hz
On-time	800 µs
Off-time	1581 µs
Duty cycle	33 %
Wave form	Triangular

Table 20 LM transmitter key parameters.

High Moment

Parameter	Value
Number of transmitter turns	12
Transmitter area	342 m²
Peak current	110 Amp
Peak moment	~500.000 NIA
Repetition frequency	30 Hz
On-time	4000 µs
Off-time	12667 µs
Duty cycle	24 %
Wave form	Square

Table 21 HM transmitter key parameters.

Figure 21 The 342 m² frame in production mode.

Receiver system

The decay of the secondary magnetic field is measured using two independent active induction coils. The Z coil is the vertical component, and the X coil is the horizontal in-line component. Each coil has an effective receiver area of 175 m² (Z), 115 m² (x).

The receiver coils are placed in a null-position:

Z coil (x, y, z) = (-13.25 m, 0.0 m, -2.0 m)
X coil (x, y, z) = (-14.65 m, 0.0 m, 0.0 m)

In the null-position, the primary field is damped with a factor of 0.01 on HM and due to PFC correction it can be neglected on LM.

Figure 22 Rudder containing the Z coil located in the top part of the tower.

The key parameters defining the receiver set up are found in Table 22.

Receiver parameters		
Sample rate		All decays are measured
Number of output gates		37 (HM) and 28 (LM)
Receiver coil low pass filter		210 kHz (Z-coil) and 250 kHz (X-coil)
Receiver instrument low pass filter		300 kHz
Repetition frequency	LM HM	210 Hz 30 Hz
Front gate	LM HM	0.0 µs 370 µs

Table 22 Receiver key parameters.

Receiver gate times are measured from the start of the transmitter current turn-off. A complete list describing gate open, close and centre times are listed in Appendix 2.

Inclination

Instrument type: Bjerre Technology

The inclination of the frame is measured with 2 independent inclinometers. The x and y angles are measured 2 times per second in both directions. The inclinometers are placed in the rear of the frame as close to the z coil as possible, see Figure 3.

The angle data are stored as x, y readings. X is parallel to the flight direction and positive when the front of the frame is above horizontal. Y is perpendicular to the flight direction and negative when the right side of the frame is above horizontal.

The angle is checked and calibrated manually within 1.0 degree by use of a level meter.

DGPS airborne unit and base stations

Chipset: OEMV1-L1 14-channe rate.
Antenna: Trimble, Bullet III GPS Antenna

The differential GPS receiver is on top of the boom in front of the frame.

The DGPS delivers one dataset per second. The raw coordinates are given in Latitude/Longitude, WGS84.

The uncertainty in the xyz-directions is ± 1 m after processing.
The processed DGPS data is combined with the EM data in the xyz-files, giving the precise position.

Key parameters of the DGPS instruments are found in Table 23.

DGPS parameters	
Sample rate	1 HZ
Uncertainty	± 1 m

Table 23 DGPS key parameters.

Altimeter

Instrument type: MDL ILM300R

Two independent laser units mounted on the frame measuring the distance from the frame to the ground, see Figure 3

Each laser delivers 30 measurements per second, and covers the interval from 0.2 m to approximately 200 m.

Key parameters of the laser instruments are found in Table 24.

Dark surfaces including water surfaces will reduce the reflected signal. Consequently, it may occur that some measurements do not result in useful values.

The altimeter measurements are given in meters with two decimals. The uncertainty is 10 - 30 cm. The lasers are checked on a regular basis against well-defined targets.

Laser parameters	
Sample rate	30 Hz

Uncertainty	10 - 30 cm
Min/ max range	0.2 m / 200 m

Table 24 Laser key parameters.

Magnetometer airborne unit

Instrument type: Geometrics G822A sensor and Kroum KMAG4 counter.

The Geometrics G822A sensor and Kroum KMAG4 counter is a high sensitivity Cesium magnetometer. The basic of the sensor is a self-oscillating split-beam Cesium vapor (non-radioactive) Principe, which operates on principles similar to other alkali vapor magnetometers.

The sensitivity of the Geometrics G822A sensor and Kroum KMAG4 counter is stated as <0.0005 nT/√Hz rms. Typically 0.002 nT P-P at a 0.1 second sample rate, combined with absolute accuracy of 3 nT over its full operating range.

Key parameters of the magnetometer airborne unit are found in Table 25.

The magnetometer is synchronized with the TEM system. When the TEM signal is on, the counter is closed. In the TEM off-time the magnetometer data is measured from 100 microseconds until the next TEM pulse is transmitted. The data are averaged and sampled as 60 Hz.

Parameter	Value
Sample frequency	60 Hz (in between each HM EM pulse)
Magnetometer on	HM
Magnetometer off	LM

Table 25 Magnetometer Airborne unit key parameters.

Magnetometer base station

Instrument type: GEM Proton.

The GEM Proton is a portable high-sensitivity precession magnetometer.

The GEM Proton is a secondary standard for measurement of the Earth's magnetic field with 0.01 nT resolutions, and absolute accuracy of 1 nT over its full temperature range.

The base station data are sampled with 1 Hz frequency.

Appendix 2: Introduction to Spatially Constraint Inversion (SCI)

Model and inversion routine

The SkyTEM data have been processed and inverted using a spatially constrained inversion (SCI) in Aarhus Workbench, a unique software package initially developed at Aarhus University, Denmark. In the SCI algorithm, a group of time-domain EM (TEM) soundings are inverted simultaneously using 1-D models (Auken et al. 2002 & 2005, Viezzoli et al. 2008). Each sounding yields a separate layered model, but the models are constrained spatially on resistivity, see Figure 23 .

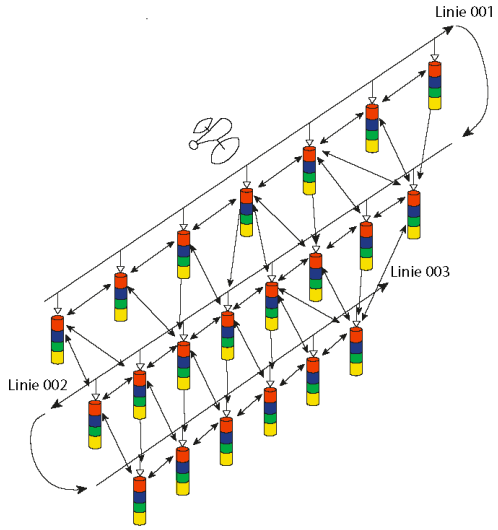

Figure 23Schematic presentation of the SCI setup. Constraints connect not only soundings located along the flight line, but also those across them (figure from hgg.au.dk).

The result of the SCI inversion is a quasi-3D model that varies smoothly along and across the profiles. The SCI inversion is capable of simultaneously inverting the interleaved HM and LM measurements, yielding a conductivity model that combines the very good shallow depth resolution offered by the low moment data and the larger depth of investigation from the high moment data.

The SCI code is run in multi-layer, smooth-model mode, in which the layer thicknesses are fixed and the data are inverted only for resistivity. The SCI smooth-model inversion typically uses 20-30 layers. Smoothness constraints are applied on the variation of resistivity with depth, in additional to the lateral constraints between adjacent models. Multi-layer smooth-model inversion is slower to compute but is usually able to provide a very close fit to the observed data.
In the model set-up the thickness of the first layer and the depth to the top of the deepest layer boundary is given. While computing the layer thicknesses, the first and last layer boundary scales the model thicknesses automatically using a log distribution.

The input data to the inversion are the LM & HM moments of the Z-component of EM data. Both moments are combined in a single inversion to increase the depth resolution. The initial model resistivity structure is a homogenous half-space model with an Auto Calculated starting resistivity.

Constraints are given as factors, i.e. a factor of 1.1 means that the parameter can vary between the starting value divided by/times 1.1 (Aarhus University).
The SCI inversion allows for horizontal and vertical constraints to be set for resistivities.
Horizontal constraints are scaled by distance using a reference distance and power function:

$$C = 1 + \left(C_{opt} - 1\right)\left(\frac{\Delta GPS}{Dist_{ref}}\right)^{n}$$

Where C is the used constraint, C_{opt} is the optimal constraint at a sounding distance of $Dist_{ref}$ and ΔGPS is the actual sounding distance.
The horizontal constraints are initially scaled by distance and a power function. Inversion for flight altitude is included after the first 5 inversion runs. The constraint on the processed flight height is set low and is only allowed a very limited variation.
The methodology for calculating the DOI is based on a recalculated Jacobian matrix from a 1D model (Christiansen and Auken, 2012). Working with global and absolute threshold values requires a relative, data-type, independent relation between the model space and data space, which we obtain by working in the logarithmic model and data spaces. For a given model, the DOI calculations solely include information from the part of the Jacobian relating to the observed data. This means that lateral or vertical model constraints or a priori information, which also contributes information to the model, is not included. The workflow includes the following steps:
1) Starting from a measured data set, the data is inverted into a smooth model. The inversion includes the data uncertainty, estimated from the data stack, and the regularization method of the chosen inversion algorithm.
2) The Jacobian for the sub-discretized model is calculated.
3) The Jacobian is finally used to compute the cumulated sensitivities from which we can deduct the DOI.

Data and noise model

The inaccuracy of TEM data is influenced by the ambient noise. This noise is reduced by selective stacking of delay time series and by applying appropriate filters in the receiver system.

Data insufficiency

For SkyTEM data, the insufficiency lies primarily in the limited delay time range that can be obtained. The earliest obtainable time gate is determined by the turnoff of the Tx current, and the latest useful time gate is determined by the signal to noise ratio. Increasing the Tx moment will give better measurements at late times, and thus improve the depth penetration, but also increase the turnoff time and thus remove

early-time gates, thereby making the near-surface resolution poorer. This trade-off is solved by transmitting an alternating sequence of (1) a low moment that can be turned off quickly to give good near-surface resolution, and (2) a high moment that will improve the signal-to-noise ratio at late times, thus improving depth penetration.

Model inconsistency

When using 1D models in the interpretation of SkyTEM data, inconsistency arises where the lateral gradient of conductivity is not small, e.g. typically in mining applications. However, also in environmental investigations, inconsistencies can arise, typically where near-surface good conductors have abrupt boundaries.
Often such inconsistency is indicated by the data residual being high and one should look upon the inversion results with some caution at these locations. 3D effects can also reveal themselves by the so-called 'pant legs', i.e. conductive or resistive structures projecting at an angle of approximately 30 degrees from the horizontal at the edges of high contrast structures.